Observation of the rock slope thermal regime, coupled with crackmeter stability monitoring: first results from three different sites in Czechia (Central Europe)

Observation of the rock slope thermal regime, coupled with crack meter stability monitoring

Ondřej Racek [1,2], Jan Blahůt [2], Filip Hartvich[2]

[1] Charles University in Prague, Faculty of Sciences, Department of Physical Geography and Geoecology, Albertov 6, 128 43, Prague, Czechia

[2] Institute of Rock Structure and Mechanics, Czech Academy of Sciences, Department of Engineering Geology, V Holesovickach 94/41, 182 09, Prague, Czechia

Correspondence to: Ondřej Racek (racek@irsm.cas.cz)

Abstract. This article describes an innovative, complex and affordable monitoring system designed for joint observation of environmental parameters, rock block dilatations and temperature distribution inside the rock mass with a newly designed 3-meter borehole temperature sensor. Global radiation balance data are provided by pyranometers. The system introduces a novel approach for internal rock mass temperature measurement, which is crucial for the assessment of the changes in the stress field inside the rock slope influencing its stability. The innovative approach uses an almost identical monitoring system at different sites allowing easy setup, modularity and comparison of results. The components of the monitoring system are cheap, off-the-shelf and easy to replace. Using this newly designed system, we are currently monitoring three different sites, where the potential rock fall may endanger society assets below. The first results show differences between instrumented sites, although data time-series are relatively short. Temperature run inside the rock mass differs for each site significantly. This is very likely caused by different aspects of the rock slopes and different rock types. By further monitoring and data processing, using advanced modelling approaches, we expect to explain the differences among the sites, the influence of rock type, aspect and environmental variables on the long-term slope stability.

This paper describes a newly designed, experimental and affordable rock slope monitoring system. By this system, three rock slopes in Czechia are being monitored for the period of up to two years. Three instrumented rock slopes have different lithology (sandstone, limestone, and granite), different aspect and structural and mechanical properties. Induction crackmeters monitor the dynamic of joints, which separate unstable rock blocks from the rock face. This setup works with a repeatability of 0.05 mm. External destabilizing factors (air temperature, precipitation, incoming and outgoing radiation, etc.) are measured by weather station placed directly within the rock slope. Thermal behaviour in rock slope surface zone is monitored using a compound temperature probe, placed inside a 3 m deep sub-horizontal borehole insulated from external air temperature. Additionally, one thermocouple is placed directly on the rock slope surface. From so far measured time series (longest one

since autumn 2018) we can distinguish differences between the monitored sites annual and diurnal temperature cycles. From the first data, the greater annual joint dynamic is measured in the case of larger blocks, however, smaller blocks are more responsive to short-term diurnal temperature cycles. The differences in the thermal regime between sites are also recognisable, and are mainly caused by different aspect, rock mass thermal conductivity and colour. These differences will be explained by statistical analyses of longer time series in the future. Moreover, we will use radiation and thermal data, to construct numerical models of rock slopes thermal-stress behaviour.

Keywords: monitoring, rock slope, stability, temperature, crack meter, horizontal borehole temperature

1 Introduction

The rock slope stability is crucially influenced by both ~~endogenous~~ rock properties and exogenous factors (D'Amato et al. 2016, Selby 1980). The rock physical properties are well known and numerous laboratory experiments and theoretical works exist in the field, however, there are very few in-situ experiments that would deal with real-world time and space scales (Fantini et al. 2016; Bakun-Mazor et al. 2013, 2020; Janeras et al. 2017; Marmoni et al. 2020). Moreover, all these studies are focused on monitoring of a single, well-known unstable rock slope.

Thermal expansion and frost action together with severe rainfall events are the main exogenous physical processes of the mechanical weathering of the rock surface (Krautblatter and Moser, 2009).~~,~~ ~~which t~~Together with chemical weathering, these ultimately result~~s~~ into ~~a~~ weakening of the rocks slopes and lowering their stability (Gunzburger et al. 2005, Vespremeanu-Stroe and Vasile, 2010; do Amaral Vargas et al. 2013; Draebing 2020). The loss of stability, caused by repeated changes in the stress field inside the rock eventually leads to a rockfall, one of the fastest and most dangerous forms of slope processes (Weber et al. 2017; Gunzburger et al. 2005). In the alpine environment, rock falls are increasingly caused by permafrost degradation and frost cracking (Gruber et al. 2004; Ravanel et al. 2017) or temperature related glacial retreat (Hoezle et al. 2017). To address the influence of permafrost melting on the rock slope stability, several monitoring systems/campaigns were proposed. Magnin et al. (2015a) constructed a monitoring system consisting of rock temperature monitoring both on the rock face and in-depth sensors. In-depth rock mass temperature monitoring is placed in up to 10m deep boreholes. The monitoring is coupled with ERT campaigns to determine sensitive permafrost areas (Magnin et al. 2015b). Girard et al. (2012), introduced a custom acoustic emission monitoring system for quantifying freeze-~~-~~induced damage in rock. Extensive monitoring system for permafrost activity in Switzerland is presented by Vonder Mühll et al., (2008) and Noetzli and Pellet, (2020). Moreover, a significant percentage of small rock falls is directly triggered by rainfall (Krautblatter and Moser, 2009; Ansari et al, 2015). The linkage between rock fall occurrence and rainfall intensity is not linear and the majority of events is triggered when rainfall intensity exceeds a specific threshold.

Among the destabilizing processes caused by changes in rock temperature and contributing to the decrease of stability are:

- rock wedging-ratcheting (Bakun Mazor et al., 2020; Pasten et al., 2015)

- repeated freeze-thaw cycles

- thermal expansion-induced strain (Gunzburger et al., 2005; Matsuoka 2008)

-and in specific conditions, exfoliation sheets can be destabilized by cyclic thermal stress (Collins and Stock, 2016; Collins et al., 2017).

~~rock wedging-ratcheting (Bakun Mazor et al. 2020; Pasten et al. 2015), repeated freeze-thaw cycles, thermal expansion-induced strain (Gunzburger et al. 2005; Matsuoka 2008) and in specific conditions, exfoliation sheets can be destabilized by cyclic thermal stress (Collins and Stock, 2016; Collins et al. 2017).~~ These processes ~~can be~~are often repeated many times~~ in specific weather conditions~~, thus effectively widening the joints and fracturing the rock. ~~Unfortunately, the last two winters in Czechia were relatively warm, which is not ideal for observing the freeze-thaw cycles. To counter this, we are currently preparing new installation in the Krkonoše Mountains (northern Czechia) at the altitude of 1270 m a.s.l. where also rock wedging-ratcheting process should be active because of the suitable disposition of newly instrumented blocks.~~

Rock slope monitoring is one of the common tasks in engineering geology, often used at construction sites ~~directly connected to the safety of large construction sites, such as dams, power plants, bridges, or tunnels~~ (Ma et al. 2020, Li et al. 2018; Scaoni et al. 2018), along roads or railways or to protect settlements. ~~Monitoring of rock slope stability can be designed using various approaches, with a background in geodesy, using GNSS or total station~~ Various approaches are used, with a background in geodesy (Gunzburger et al. 2005; Reiterer et al. 2010; Yavasoglu et al. 2020), geotechnics ~~with crack meters, inclinometers and extensometers~~ (Greif et al. 2017; Lazar et al. 2018), geophysics ~~with ambient vibration monitoring, ERT profiling and micro seismical sensors~~ (Burjanek et al. 2010; 2018; Weber et al. 2018; Coccia et al. 2016; Yan et al. 2010; Weigand et al. 2020; Warren et al. 2013), or remote sensing methods~~, such as TLS (Terrestrial Laser Scaner), UAV (Unmanned Aerial Vehicle) or ground based photogrammetry or GB InSAR (Ground Based Interferometric Synthetic Aperture Radar)~~ (Sarro et al. 2018; Matano et al. 2015).~~These systems using various types of sensors (Fantini et al. 2017, Janeras et al. 2017). Measurement of air temperature, accelerometers, cameras and seismographs are often used to detect and explain rock fall events~~ Most commonly, sensors such as thermometers, , accelerometers, inclinometers, visible light or IR cameras, total stations, TLS, GbSAR and seismographs are used to detect potential rock fall events (Burjanek et al. 2010, 2018; Tripolitsiotis et al. 2015; Matsuoka, 2019). ~~The use of these methods is more suitable for monitoring larger parts of rock slope and allows spatiotemporal identification of rock fall events.~~ These methods are more suitable for monitoring large rock slopes. ~~On the other hand, t~~ Tiltmeters~~ and~~, extensometers and other geotechnical devices are usually used to ~~single unstable block/part of rock slope monitoring~~ monitor a single unstable block/part of rock slope (Barton et al. 2000; Lazar et al. 2018). To quantify the influence of meteorological variables, weather station should be included within monitoring systems. Rarely, environmental monitoring is supplemented by solar radiation monitoring (Gunzburger and Merrien-Soukatchoff, 2011). ~~These point measuring methods can describe spatial changes of a monitored feature with higher accuracy, however, the use of these devices does not allow to monitor larger parts of rock slope.~~

~~Complex monitoring systems are used to monitor potentially unstable rock slope parts. Janeras et al. (2017) introduced a multi-technique approach of rockfall monitoring of unstable mass. The system consists of crack meters, TLS, GB InSAR and total station surveying. Jaboyedoff et al. (2004) used geodetic network, extensometer network and weather monitoring. Vaziri et al. (2010) presented a review of monitoring techniques for open-pit mine walls monitoring. Carla et al. (2017) used GB InSAR to monitor displacement of mine slopes failures. Large rock slides are monitored by Crosta et al. (2017) using GB InSAR, Satelite InSAR and borehole inclinometry. Loew et al. (2012) used borehole inclinometry and borehole extensometry combined with GB InSAR interferometry in the large Randa rockslide monitoring. Zangerl et al. (2010) used total station measurements, coupled with borehole inclinometers for a similar purpose. Long-term rock slope destabilization is monitored using total station measurements, multipoint surface extensometers, borehole inclinometers (Chen et al. 2017), or TLS measurements eventually (Hellmy et al. 2019). Usually, these monitoring systems are designed as experimental, aiming to develop new early-warning sensors or approaches (Loew et al. 2017; Jaboyedoff et al. 2011) or to describe processes of rock slope destabilization (Fantini et al. 2016; Kromer et al. 2019; Du et al. 2017). However, these systems are site-specific and installation of a similar system on more sites is complicated and financially demanding.~~

Usually, approaches and sensors are combined. Large rockslides are monitored by Crosta et al., (2017), Zangerl et al., (2010) and Loew et al., (2012) using combination of remote sensing, geodetical network and borehole inclinometry. Experimental monitoring systems aim to develop or test new sensors or approaches (Loew et al., 2017; Jaboyedoff et al., 2011; Chen et al., 2017; Hellmy et al., 2019) or to describe long term processes of rock slope destabilization (Fantini et al., 2016; Kromer et al., 2019; Du et al., 2017). However, these systems are site-specific and installation of a similar system within multiple sites is complicated and often financially demanding.

~~These systems are sometimes complemented with environmental data observations. However, these~~ Thermal observations are often limited to air temperature and/or rock face temperature monitoring only (Jaboyedoff et al. 2011, Blikra and Christiansen, 2014; Marmoni et al. 2020; Collins and Stock, 2016; Collins et al. 2018; Eppes et al. 2016). Less commonly, the temperature ~~is~~ changes are measured ~~in~~ within the rock mass depth (Magnin, et al. 2015a, Fiorucci et al. 2018). ~~The absence of precise data about temperature changes in rock mass depth makes the assessment of the thermally-induced stress field response inside the rock mass complicated. Without in-depth temperature data and incoming radiation, the determination of heating/cooling trends causing internal volume and stress field changes is difficult. Also, the monitoring systems are usually designed specifically for the monitored sites, which brings difficulties for generalization of the results or installation of the system at more sites.~~ Site-specific designed systems are difficult to modify and usually expensive. This brings difficulties into data processing because they are locally biased and cannot be directly compared.

~~Therefore, we have designed an easy to modify monitoring system, which measures the physical parameters in a 2D environment in the field conditions, both on the rock face and inside the rock mass. With just minor modifications we can instrument various rock slope sites.~~

Therefore, an easy-to-modify, modular and affordable monitoring system composed of crackmeters, weather station, solar radiation and compound borehole temperature probe has been designed and tested. With just minor modifications, various rock slope sites can be easily instrumented, allowing to compare data about rock slope temporal behaviour in different settings. Which we are expecting will bring new, much needed data about rock slope stability spatio-temporal development (Viles, 2013).

2 Monitoring methods

The ~~monitoring~~ rock slope monitoring methods ~~mentioned in introduction~~ have recently gone through a massive development concerning precision, accuracy, reliability, sampling rate, and applicability (Tables 1, 2). Even completely new methods were established, for example, ~~UAV~~ unmanned aerial vehicles applications, TLS, etc. This expansion was mostly allowed by the rapid development of corresponding fields of informatics, computation technologies, communication channels and satellite technology applications.

Unlike to above-mentioned systems, the monitoring system ~~which we are presenting~~ presented here (Fig. 1,2; Table 1), can be placed at various sites without major modifications. Using common safety rules and methods for working in heights, the system can be placed directly within vertical or even overhanging rock face. Anchoring ~~for system installation~~ must be placed within a stable part of the rock slope, which ensures worker´s safety under any circumstances. This monitoring design brings an opportunity to compare results from different locations and observe generally applicable regularities in rock face thermo-mechanical behaviour thanks to the ~~similar~~ same~~monitoring methodology~~ instrumentation on various rock slope sites. ~~Our monitoring system (Table 1, Fig. 1) is composed of the following components:~~ All sensors are calibrated by manufacturer, before are installed on rock slope to provide precise data. The monitoring system (Table 1, Fig. 1) is composed of the following components:

~~a set of automatic induction crack meters, coupled with dataloggers (Fig. 1) measuring relative block displacement~~

- ~~a environmental station with a set of sensors measuring various meteorological data (Fig. 1), such as air temperature, humidity and pressure (Table 1), and global radiation balance of the rock face (Fig. 4) using pair of pyranometers~~
- ~~a set of 12 thermometers placed along a 3 m deep borehole, carefully insulated between each neighbouring sensors, measuring rock slope thermal depth profile at ten minutes interval~~
- a set of automatic induction crack meters, coupled with dataloggers (Fig. 1) measuring relative block displacement
- a weather station with a set of sensors measuring various meteorological data (Fig. 1), such as air temperature, humidity and pressure (Table 1), and rock slope surface solar radiation balance (incoming/reflected radiation) of the rock face (Fig. 5) using pair of pyranometers

- a set of 12 thermocouples placed along a 3 m deep borehole (Fig 2.), carefully insulated between each neighbouring ~~sensors~~sensor, measuring rock slope temperature in-depth profile

Component	Manufacturer	Accuracy	Resolution	Repeatability	Measuring range	Max sampling rate	Protection	Operational temperature	Service life	Price
Crackmeter Gefran PZ 67-20	GEFRAN (It)	<0.1 %	0.05 mm	0.01 mm	0-200 mm	N/A	IP67	-30 - 100 °C	> $25*10^8$ m strok	300 €
Datalogger Tertium Beacon	Tertium tech. (It)	N/A	N/A	N/A	N/A	< 1 sec	IP65	-30 - 60 °C	> 5 years	190 €
Datalogger Temp. Sensor	Tertium tech. (It)	0.02 °C	0.01 °C	N/A	-30 - 60 °C	< 1 sec	IP67	-30 - 60 °C	> 5 years	
Control unit, battery, solar p	FIEDLER (Cz)	N/A	0.00X; 16bit	N/A	N/A	1 min	IP66	-30 - 60 °C	> 5 years	
Temperature sensor	FIEDLER (Cz)	0.1 °C	0.1 °C	0.01° C	-50 - 100 °C	1 min	IP66	-50 - 100 °C	> 5 years	
Rain gauge SR03 500cm2	FIEDLER (Cz)	0.05 mm	0.1 mm/year	0.1 mm	N/A	50 m. sec	IP66	0 - 60 °C	> 5 years	1 650 €
Humidity sensor	FIEDLER (Cz)	0.008 %	< 0.1 %/year	0.02 %	0 - 100 %	1 min	IP66	-50 - 100 °C	> 5 years	
Atmospheric pressure sensc	FIEDLER (Cz)	2 mbar	0.025 mbar	0.1 mbar	300 - 1100 mbar	1 min	IP66	-40 - 70 °C	> 5 years	
Pyranometer SG002	Tlusťák (Cz)	10%/day	20 μV/Wm^2	< 5%	300 - 2800 nm (0 - 1200 W/m^2)	1 min	IP66	-30 - 60 °C	> 5 years	450 €
Borehole temperature sens	FIEDLER (Cz)	0.1 °C	0.1 °C	0.01° C	-50 - 100 °C	1 min	sealed inside	-30 - 60 °C	> 5 years	1 150 €
Datastorage/procesing	FIEDLER/SigFox	/	/	/	/	1 hour	/	/	infinite	200 €

Table 1: List of presented monitoring system components, with performance metrics and prices.

All the elements of the system (Table 1) are commercially available at affordable expenses (one site instrumentation costs approx. 5000 Eur~~) (Table 1)~~, and are easy to replace by even moderately experienced user. Additional costs are drilling works (1-2 000 EUR). Cost of drilling works depends on the site accessibility and rock mass hardness. The price of the specific monitoring system is also affected by the number of used crack meters and data loggers. On the other hand, system maintenance costs are not higher than 300 Eur per year including data transmission, processing and storage. This makes system ideal to use on multiple sites, without great financial demands. When using the same instrumentation, data from different rock slope sites can be compared and analysed to better understand general rock slope spatio-temporal behaviour.

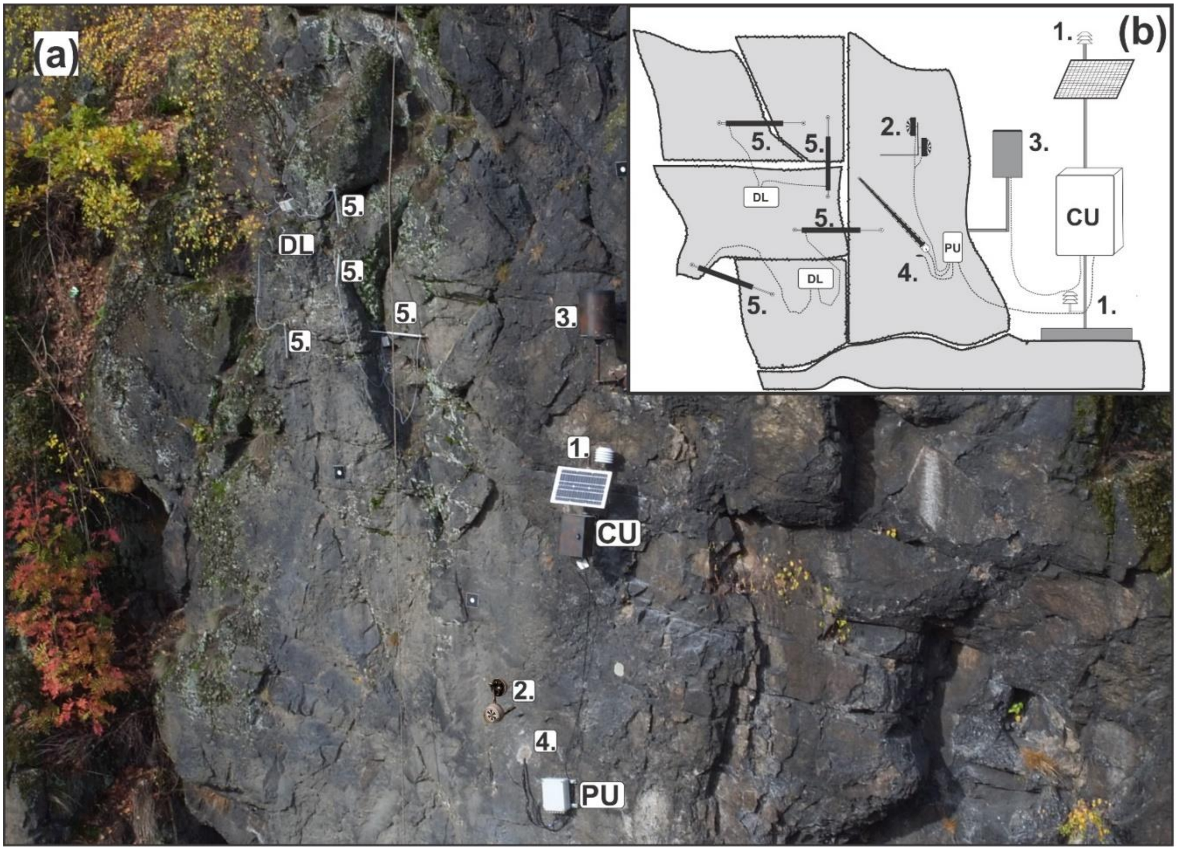

Figure 1: Photo of actual monitoring system at Tašovice site (a). Generalized scheme of the monitoring system (b). CU: control unit, PU: processing unit, DL: data logger, 1.: Temperature sensor, 2.: Pyranometers, 3.: Rain gauge, 4.: Borehole compound temperature ~~monitoring~~probe, 5.: Crack meters (only four of total six crack meters are visible on this photo)

2.1 Dilatation monitoring

At each site, suitable joints separating unstable rock blocks were selected. ~~Joints were selected to best represent general directions of expected rock blocks movements.~~ Joints and subsequent crackmeter placement were selected to best represent general directions of expected rock blocks destabilization direction. Where it was possible, joints that directly separate unstable block from ~~rock slope~~stable rock were chosen. These joints were afterwards instrumented with calibrated ~~automatic~~ induction crack meters Gefran PZ-67-200.~~, working on the induction principle.~~ Crack meters can record movements smaller than 0.1 mm (Tables 1,2). In comparison with other methods measuring spatial change, their precision is high, with lower costs (Table 2). The temporal resolution of the measurement is nearly continuous when the crack meter position can be read every second (Table 2). Moreover, we have tested these in a controlled temperature environment using a climate chamber to find out any temperature-dependent errors. In this controlled test, we were able to measure the expansion of a concrete block. The resulting block expansion measurements matched theoretically calculated concrete block expansion. This way we made sure, that measurement of the crack meters is not biased by dilatation of the device itself. ~~These c~~Crack meters are suitable for harsh conditions (Table 1)., Device can standwhere are affected by temperature changes, snow cover, ice accumulation or rainfall with IP 67 protection.. The protection level of crack meters is IP67. These crack meters work with good measurement accuracy (Table 1) (GEFRAN, 2019). Crack meters are coupled with Tertium TAG Beacon dataloggers (Tertium technology, 2019), which also contain accurate in-situ temperature sensors (Table 1). When a datalogger is placed within the discontinuity, the local temperature microclimate can be estimated.records local temperature The joint dilatation and temperature data are stored in the datalogger and can be wirelessly transmitted at a distance of up to a hundred meters using wi-fi, which simplifies data collection as it can be usually performed from below the rock face. Tertium BeaconTAG data can be sent to a server via IoT SigFox network. The crack meters and dataloggers are powered with two AA batteries, which last typically 6-12 months according to local climate. The displacement and temperature are set to be measured every hour. This can be however remotely changed if necessary, for example during special experiments such as thermal camera monitoring campaigns (Racek et al. 2021). Precision of crack meters allows to monitor small movements in great temporal scale, which cannot be achieved using repeated remote sensing or geodetical campaigns (Table 2).

Method	Results	Range	Precision	Sampling rate	Online data	Price
Induction crack meter	1D distance	< 1 m	0.01 mm	seconds-days	yes	300 €
Precision tape	1D distance	< 30 m	0.5 mm/30 m	hours-days	no	800 €
Fixed wire extensometer	1D distance	10 - 80 m	0.3 mm/30 m	hours-days	yes	4 000 €
Rod for crack opening	1D distance	< 5 m	0.5 mm	hours-days	no	300 €
LVDT	1D distance	< 0.5 m	0.25 mm	seconds-days	yes	170 €
Laser dist. meters	1D distance	< 1000 m	0.3 mm	seconds-days	yes	1 500 €
Portable rod dilatometer	1D distance	< 1 m	0.1 mm	hours-days	no	350 €
Total station triangulation	3D distance	< 1000 m	5 - 10 mm	hours-days	yes	3 000 €
Precise levelling	1D distance	< 50 m	< 1 mm	days	no	350 €
EDM	1D distance	1 - 15 km	1 - 5 mm	minutes - days	no	10 000 €
Terestrial photog.	3D distance	< 100 m	< 20 mm	hours-days	yes	1 000 €
Aerial photog.	3D distance	< 100 m	10 - 100 mm	days	no	1 500 €
Tiltmeter	inclination change	±10°	0.01°	seconds-days	yes	300 €
GPS	3D distance	Variable	< 5 mm	seconds-days	yes	2 000 €
TLS	3D distance	Variable	5 - 100 mm	hours-days	yes	100 000 €
GB InSAR	3D distance	Variable	< 0.5 mm	hours-days	yes	100 000 €

Table 2: A comparison of rock slope spatial change monitoring techniques (updated after Klimeš et al., 2012)

2.2 Environmental monitoring

For the monitoring of the environmental weather and climatic parameters at the study sitessites of interest, we use automatic environmental weather stations manufactured by Fiedler environmental systems. These are composed of registration, communication and control unit M4016-G, external tipping-bucket rain gauge, two temperature sensors, atmospheric pressure sensor, humidity sensor, and a pair of pyranometers, measuring the ~~global radiation~~incoming and reflected solar radiation. All these sensors and the control unit are powered by a 12 V battery, which is charged by a small solar panel (Fig. 1). Except for precipitation, which is measured ~~continuously~~ using a pulse signal, all other ~~climatic~~ meteorological variables and solar radiation are measured every 10 minutes. The control unit is equipped with a GSM modem, which sends the data automatically to the server of the provider every day. For information about accuracy, durability and price of environmental monitoring see table 1.~~. To expand the spatial extent of temperature data, thermal camera time-lapse campaigns were performed and are also planned in future (Racek et al. 2021).~~

To compute the radiation balance (incoming minus reflected solar radiataion) of a rock face, it is necessary to measure ~~both incoming and reflected radiation~~ with two opposite facing pyranometers. For this purpose, a set of pyranometers is used (Gunzburger and Merrien-Soukatchoff, 2011; Janeras et al. 2017; Vasile and Vespremeanu-Stroe, 2017). Pyranometers are placed perpendicular to the rock face, one facing the rock surface while the other the sky hemisphere. ~~Our monitoring system uses two pyranometers placed perpendicular to the rock face, one facing the rock surface while the other the sky hemisphere.~~ This setup enables to measure both incoming and reflected solar radiation. The sensors are not placed directly on the rock face, but on an L-shaped holder, which allows placing both sensors almost at the same point (Fig. 2). The rock-facing pyranometer is placed at a distance of approx. 10 centimetres from the rock surface. The pyranometers ~~(type SG002) are supplied by Fiedler environmental systems company (FIEDLER, 2020), and~~ have an output of 0–2 V, which corresponds to global radiation of 0–1200 W/m^3, the monitored wavelength spans from 300 to 1200 W/m^2~~nm~~. Monitored wave length spans from 300 to 2800 nm. Outputs from pyranometers are processed by a converter and then ~~send to the control unit, to be~~ sent with the other monitored meteorological variables to the data hosting server.

2.3 Borehole temperature monitoring

For the ~~complex~~ monitoring of the thermal behaviour of a rock slope, it is necessary to know temperatures at different depths of the rock mass. ~~This is a crucial and innovative part of our monitoring system. Temperature from rock mass depth contributes to a better understanding of the rock slope thermal regime.~~ The newly designed in depth compound temperature probe (Fig. 2) is a crucial part of our monitoring system.

The sensors are placed in a 3 m deep sub-horizontal borehole. ~~The borehole is drilled close to the monitored unstable rock blocks. However, t~~To ensure safety during drilling and the long lifespan of borehole and sensors, the borehole itself is drilled to the stable part of the rock slope.~~, perpendicularly to the surface.~~ The borehole is then equipped with a custom-designed ~~device~~ probe with a set of ~~temperature sensors~~thermocouples.~~,~~ ~~placed along a tubular spine at different depths.~~ Technical parameters of temperature sensors are the same as for air temperature sensors (Tab 1). Thermocouple sensors that are connected to copper rings are originally designed for soil temperature measurement. ~~Copper rings with 5 cm diameter, connected to thermal sensors, are placed at a given distance on the tubular spine (5 cm below the surface, 10 cm, 20 cm, 30 cm, 50 cm, 75 cm, 100 cm, 150 cm, 200 cm, 250 cm and 300 cm). Additionally, one temperature sensor is placed directly on the rock surface. The head of the borehole is insulated, to prevent air and water inflow into the rock, and the sensors inside the~~

~~borehole are separated by thorough thermal insulation, to ensure the temperatures are not affected by the air circulation in the borehole.~~ By connecting these to copper rings, they are suitable to measure temperature of borehole walls. Copper rings with 5 cm diameter are placed at a given distance on the tubular spine (5 cm below the surface, 10 cm, 20 cm, 30 cm, 50 cm, 75 cm, 100 cm, 150 cm, 200 cm, 250 cm and 300 cm). Probe is placed in the sub-horizontal borehole, so copper rings containing temperature sensors lay directly on borehole walls (Fig. 2) By that it is ensured that probe is measuring directly rock mass temperature. Additionally, one thermocouple is placed directly on the rock slab surface (Fig. 2). The head of the borehole is insulated, to prevent air and water inflow into the rock, and the sensors inside the borehole are separated by thorough thermal insulation, to ensure the temperatures are not affected by the air circulation in the borehole. This way, temperature readings from borehole compound probe corresponds with in situ rock mass temperature. The thermal data, collected every 10 minutes, are passed through a converter and send to the main control unit of the environmental station.

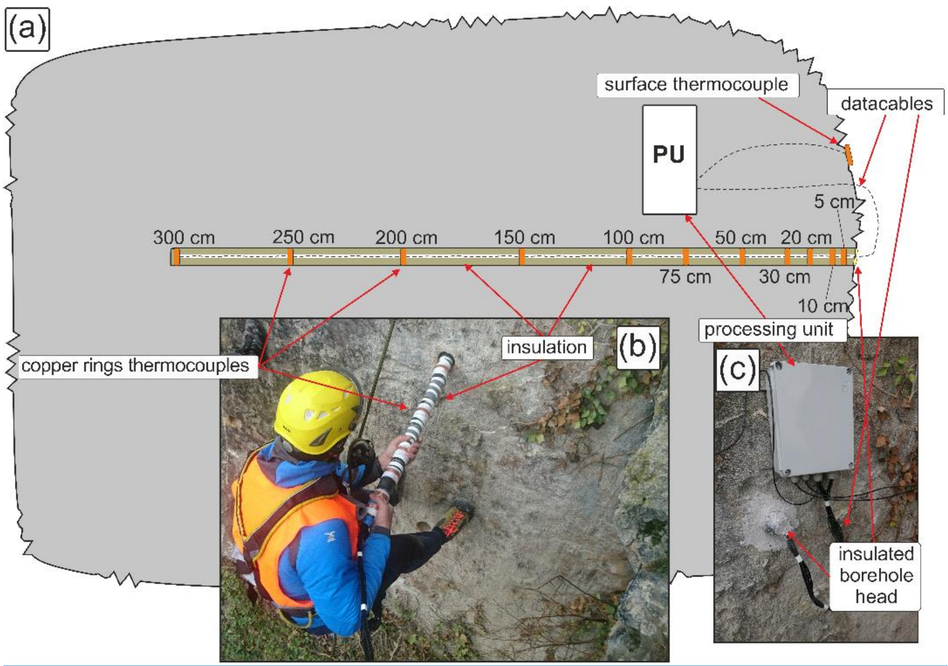

Figure 2: Compound borehole thermocouple probe. (a): generalised scheme, (b): photo of compound thermocouple probe installation, (c): insulated head of sub-horizontal borehole with processing unit.

3 Instrumented sites

The monitoring system has been so far established at three different sites (Fig. 3~~2~~), using the same instrumentation set~~-~~up. The sites were chosen deliberately in steep rock slopes built of various rock types, with various aspect, diverse geological history (Fig. 3).~~ and, t~~To integrate a practical applicability side~~, at~~ locations where the potential rockfall endangers buildings, infrastructure or other social assets were chosen.

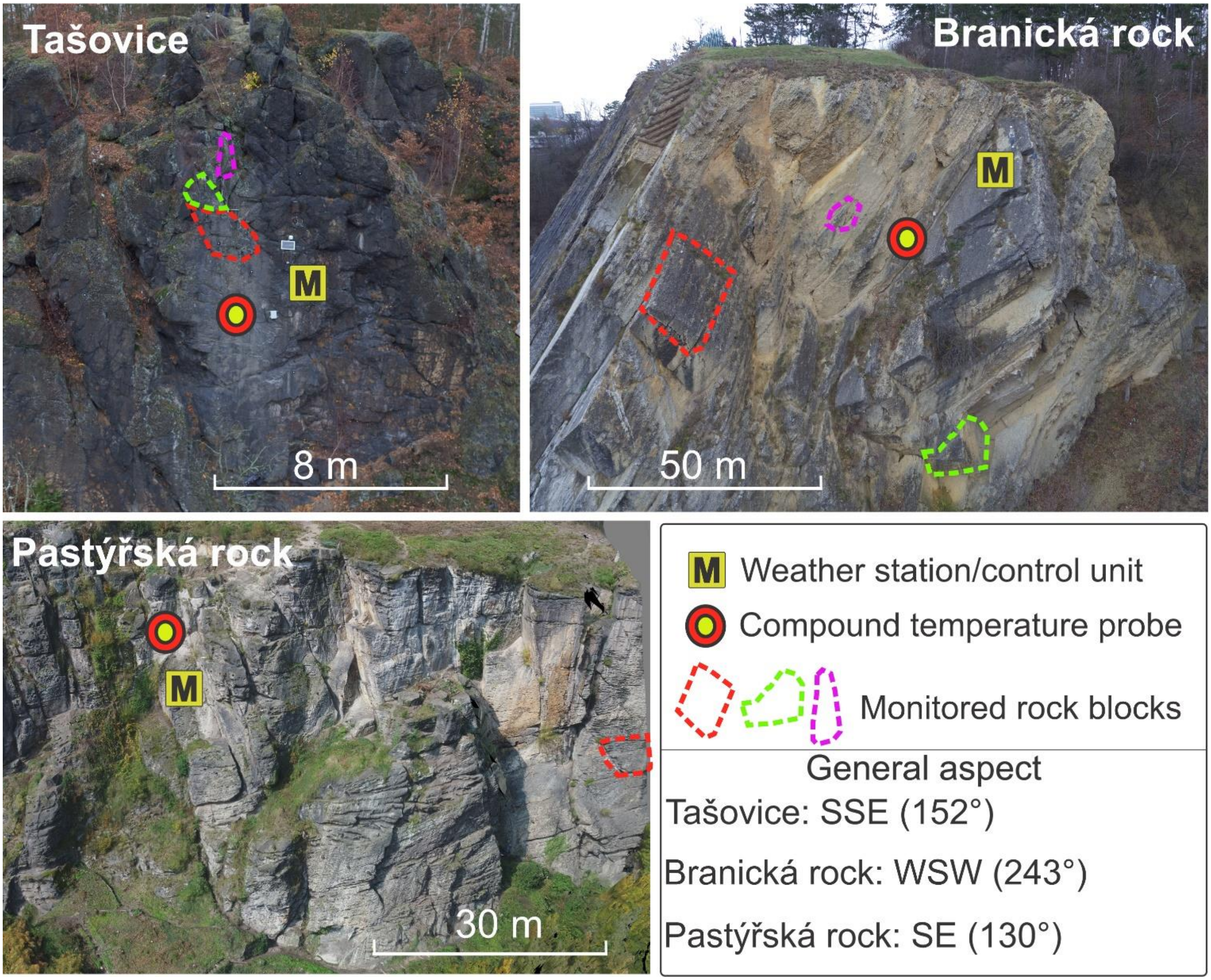

Figure 32: ~~Overview of three so far instrumented sites. Position of atmospheric monitoring and 3 m thermometer borehole. By different colours are indicated monitored rock blocks.~~ Three instrumented rock slope sites. On each photography are indicated monitored rock blocks (different colour), compound borehole temperature probe and weather station position.

3.1 Pastýřská rock (PS)

The first instrumented rock slope (Fig. 32) called "Pastýřská rock" is located on the Elbe riverbank in Děčín town, NW Czechia. Monitoring of meteorological variables was started in late 2018 (Table 5.), followed by crack meters installation and in-depth borehole temperature probe~~sensor~~. Pastýřská rock is formed by Cretaceous sandstone, with a general southeast orientation. The mechanical and physical properties of sandstone samples are listed in table 32. The rock slab with pyranometers and borehole is dipping 87° towards the east (085°). On this site, ~~using traditional methods,~~ three main discontinuity sets were identified using compass measurements (Table 3). (Table 4). This locality was known for extensive rock fall activity in past, which lead to rock slope stabilization works in the late 1980s. However, the block monitored by the crack meters remained in its natural state., without any stabilization measures. At this site, one block is monitored, using two pairs of crack meters (Table 5). This partial block has dimensions of 6.7 x 10.7 x 2.5 m. Monitoring at this rock slope has been in operation since autumn 2018. The monitored block is located in the overhanging part of the rock slope and all four visible cracks are monitored. The colour of the rock slope surface varies from dark, to light grey (Fig. 32). The rock slab, where the pyranometers are placed is coloured in light grey colour.

3.2 Branická rock (BS)

This rock slope (Fig. 23) in Prague (Central Czechia) was instrumented in summer 2019. This rock slopeand is formed by several Silurian and Devonian limestone layers, with varying mechanical and physical properties (Table 32). The rock slope was artificially created by blasting and used till the 1950s as a limestone quarry. The rock slope is located on a Vltava riverbank and it is generally facing west-south-westwards. The pyranometers and the borehole temperature sensors are placed on a rock slab dipping 80° to the southwest (235°). Three main discontinuity sets were identified using a geological compass at Branická rock site (Table 3). The site was known for extensive rock fall activity in the past, even after quarry closing, which resulted in partial stabilization of most known unstable blocks in the 1980s. At this site, three unanchored blocks (Fig. 32) are monitored with seven crack meters (Table 6). In the upper part of the rock slope lies the largest monitored block at this site, with dimensions 0.9 x 4.5 x 3.7 m. This block is monitored with three crack meters. The second block is located at the bottom part of the rock slope, partly shaded by vegetation. Dimensions of the second block are 2.5 x 1.6 x 3.6 m. The second block slowly slides on the bottom surface and is instrumented with two crack meters. Finally, the third monitored block is smaller (0.8 x 1.4 x 0.4 m). It is located in a highly weathered part of rock slope and monitored with two crack meters. Monitoring at Branická rock site is running since autumn 2019 (Tables 5, 6). The colour of limestone varies from grey to yellow (Fig 23) and the colour of limestone facing pyranometer is light grey.

3.3 Tašovice (T)

The third instrumented site (Fig. 32) is a rock slope above a local road and Ohře river near Karlovy Vary town, W west Czechia. Rock slope is formed by partly weathered granite with varying mechanical and physical parameters properties (Table 23). Generally, it is facing south-south-east direction (Fig. 3). The instrumented slab is dipping 88° to the south (170°). At this site, three relatively poorly developed discontinuity systems were identified using a geological compass in the field (Table 3). At this site, small rock falls are frequent as it can be seen from the fresh rock and debris accumulation under the rock face. The locality was fully instrumented with borehole temperature sensors probe, environmental station and global radiation monitoring in spring 2020. Three relatively small blocks are monitored at this site. Block 1 (1.7 x 1 x 2.1 m), Block 2 (0.9 x 0.8 x 0.4 m) and Block 3 (0.5 x 1.2 x 0.4 m). Each block movement is monitored with a pair of crack-meters. The colour of the rock slope varies from black to dark grey. The granite surface at the pyranometers site has dark grey colour (Fig. 3).

4 Fieldwork campaigns

Each instrumented rock slope, was characterized using traditional geological, geomorphological and geotechnical methods, such as measuring geometrical properties of joints and fault planes, relative surface strength measurement using a Schmidt hammer, discontinuity density measuring, and stability assessment estimated using geotechnical classifications (Racek, 2020). ~~Mechanical and physical properties of the rocks were determined by common laboratory tests, using collected representative rock samples (Table. 2).~~ Mechanical and physical properties of rock samples (Table 3) will serve as inputs to numerical models of thermally induced strain constructed using Multiphysics ELMER (Raback and Malinen, 2016) and FEATool (FEATool, 2017) software.

site	samples	ultrasound testing (wet samples)					pressuremeter (dry samples)					Brazilian test (dry samples)	
		ρ [g/cm^3]	E [GPa]	v [GPa]	v	K[GPa]	hardness [MP	E [GPa]	μ [GPa]	v	K [GPa]	Fmax [kN]	σ_{rt} [MPa]
Pastýřská rock - sandstone	unweathered	1.87 - 1.92	13.8 - 17.4	5.8 - 7.7	0.12 - 0.26	6.6 - 10.4	22.3 - 28.5	14.8 - 17.2	6.2 - 6.9	0.17 - 0.24	7.6 - 11.2	3.0 - 5.5	1.3 - 2.4
	weathered	1.81 - 1.99	8.5 - 15.8	3.7 - 6.3	0.14 - 0.28	4.1 - 11.9	3.9 - 11.0	2.2 - 6.0	1.0 - 2.4	0.24 - 0.39	3.9 - 4.0	0.7 - 3.6	0.3 - 1.6
Branická rock - limestone	unweathered	2.68 - 2.69	75.1 - 79.6	29.2 - 30.8	0.28 - 0.29	58 - 61.9	77.1 - 244.6	65.8 - 75.0	24.9 - 29.0	0.28 - 0.41	50.7 - 129.7	14.1 - 36.1	5.9 - 15.6
	weathered	2.67 - 2.69	73.4 - 78.1	27.9 - 30.2	0.29 - 0.34	62.2 - 64.3	88.2 - 170.5	63.6 - 73.1	24.4 - 28.2	0.27 - 0.31	49.3 - 61.0	18.1 - 33.4	7.8 - 14.0
	with cracks	2.67 - 2.69	64.5 - 78.4	24.4 - 30.3	0.29 - 0.32	60.4 - 63.4	52.1 - 192.3	25.4 - 74.0	9.6 - 27.9	0.27 - 0.33	24.7 - 61.2	11.4 - 26.9	4.7 - 10.9
Tašovice - granite	weathered	2.39 - 2.52	5 - 11.9	1.8 - 4.2	0.39 - 0.42	7.6 - 22.7	36.1 - 63.1	4.3 - 15.0	1.6 - 5.6	0.27 - 0.41	4.4 - 20.4	6.5 - 11.2	2.4 - 5.0

~~Table 2: Mechanical and physical properties of laboratory tested rock samples from all three monitored sites.~~ Table 3 Mechanical and physical properties of laboratory tested rock samples from all three monitored sites. ρ: density, E: Young´s modulus, v: Poisson´s ratio, μ: shear modulus, K: bulk modulus, Fmax: maximal axial force, σ_{rt}: max tensile strenght

Traditional methods ~~are~~ were supplemented with state-of-the-art methods of rock slope analysis, including analyses of 3D point clouds and derived mesh surfaces, based on SfM (structure-from-motion, a computerized photogrammetric technique based on the calculation of 3D point cloud from overlapping photos with varying focal axis orientation) (Westoby et al. 2012) processing using the data collected with a UAV or TLS collected data. The obtained detailed rock surface models are then analysed using Cloudcompare and its plugins (Girardeau-Monaut, 2016; Thiele et al. 2018; Dewez et al. 2016) and DSE software (Riquelme et al. 2014) to derive the joint and fault planes and measure their spatio-structural properties (Fig. 4). ~~Moreover, three main discontinuity systems that were identified using a geological compass in the field at all three sites are summarized in Table 3.~~ Discontinuity sets defines partial blocks which forms rock slopes surface.

Discontinuity sets	Pastýřská rock	Branická rock	Tašovice
System 1	80/040	50/325	50/090
System 2	86/310	90/197	50/220
System 3	80/275	62/085	88/345
System 4	30/180	62/210	46/181

Table ~~3~~4: Three main discontinuity sets identified in the field using geological compass. Dip/Dip direction

~~Point cloud data, that were produced by UAV SfM photogrammetry were analysed, edited in Cloud Compare and afterwards principal poles (Fig. 3) were automatically identified using DSE software (Riquelme et al. 2014).~~

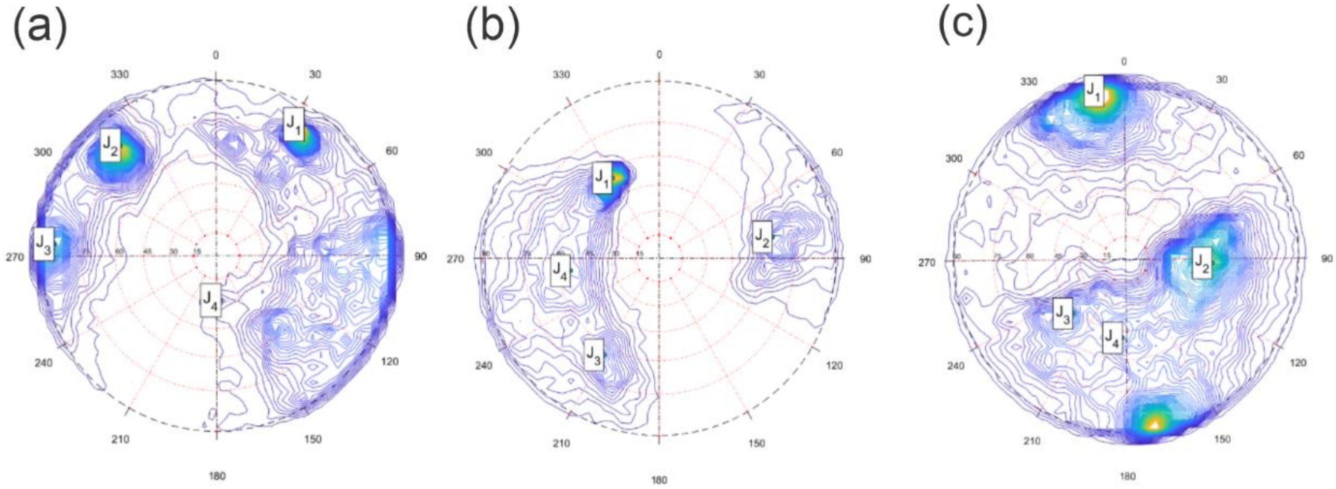

Figure ~~3~~4: Principal poles density, with four main discontinuity sets (J1 – J4) classified using DSE software (Riquelme et al. 2014). Density of principal poles corresponds to main discontinuity sets identified from pointclouds. (a): Pastýřská rock, (b): Branická rock, (c): Tašovice

5 First results

The monitoring systems are operational ~~from~~ for 1 to 2 years. During most of the period, the gauges and sensors operated without problems or interruptions. However, some accidents or breakdowns occurred, the most serious being the destruction of one pyranometer by ~~boulders~~debris, washed down by a rainstorm. As the experimental sites are easy to reach and spare parts easy to obtain, any broken or damaged elements can be replaced within a few days. ~~Workers within rock faces are using safety gear, such as full-body harness and helmet. Securing is done with static ropes and working grade brake. In the case of Pastýřská rock, workers can use Via Ferrata routes.~~

From the discontinuity analyses it is visible (Fig. 4, Table 4.), that in the case of Pastýřská and Branické rocks the discontinuity systems are clearly defined. Discontinuity sets are in the case of these sites defined mainly by sedimentary layers and cracks perpendicular to them. In case of Tašovice, discontinuity systems are less pronounced. On this rock discontinuities are linked mainly with tectonically predisposed weak zones and weathered parts of granite rock. Mechanical properties of rock mass samples differ significantly according to degree of weathering (Table 3). Best results in case of hardness were measured for unweathered limestone from Branická rock site. The lowest hardness shows weathered sandstone from Pastýřská rock site. At Tašovice, due to degree of weathering of whole rock slope, we ware not able to collect unweathered samples.

5.1 Environmental monitoring

Environmental Weather station monitoring on all instrumented sites works without problems. From measured time-series of meteorological variables (Table 45) rock slope microclimate can be defined. Also, the influence of these on monitored discontinuities position can be determined. . From these, the influence of these on the monitored discontinuities position can be determined using statistical analyses. Comparison of crack opening with measured rainfall events using simple graph does not indicate any visible influence of precipitation on the crack opening/closing. However, the measuring period is still short, with prevailing dry, relatively warm weather. Conversely, there is a visible influence of air and rock mass temperature to block dilatation (Racek et al., 2021), where both diurnal and annual cycles can be identified (Fig. 96). Basic statistical data descriptions of measured environmental meteorological variables are listed in Table 5.

Site	Active since	Active days	Rainfall [mm]	Temp. [°C]			Pressure [hPa]			Humidity [%]		
			sum	min	max	mean	min	max	mean	min	max	mean
Pastýřská rock	25.01.18	1098	1503	-9	41.2	10.5	963.5	1026.4	996.9	13.3	96.1	72.9
Branická rock	21.05.19	617	1020	-7	44	13.2	955.3	1017.4	987.4	12.5	95.8	70.4
Tašovice	12.12.18	777	691	-10	45.5	10.4	935.3	997.1	968.8	17.4	96.7	76.4

Table 5: Overview of measured meteorological variables at all three sites. The last measurements considered were measured on 27.1.2021.

5.2 Rock surface radiation balance

Monitoring of rock face surface solar radiation balance was installed at monitored rock slopes during 2020 2020 (Branická rock: 1/2020, Pastýřská rock 2/2020; Tašovice 12/2020)., therefore we still miss a full-year global radiation cycle. Even from these incomplete data we can observe the differences between individual sites (Fig. 54). Basic statistical description of so far measured data is listed in table 5. Local conditions influence incoming radiation pattern by general aspect of the rock slope (temporal shift of incoming radiation peak), rock slope albedo or by shading effect of pyranometer´s surroundings. Differences in the absolute reflected radiation are mainly caused by the different colour of rock faces, by different heating and cooling trends of the rock mass and by the different angle of incoming solar radiation caused by the aspect of the instrumented slab.

	Radiation incoming [W/m²]			Radiation reflected [W/m²]		
	Pastýřská rock	Branická rock	Tašovice	Pastýřská rock	Branická rock	Tašovice
Mean	85.9	156.7	34.9	25.0	85.9	2.9
Variance	38896.8	53102.1	8910.6	2304.4	10907.8	111.5
Stdev	197.2	230.4	94.4	48.0	104.4	10.6
Median	0.0	20.3	9.4	0.0	0.0	0.0
Q_3	54.5	189.6	20.3	15.0	160.0	1.1
Q_1	0.0	4.6	8.7	0.0	2.3	0.0
Min	0.0	0.0	0.0	0.0	0.0	0.0
Max	1198.8	1197.3	1052.3	413.9	910.0	119.1

Table 5: Basic statistical description of pyranometers measured data.

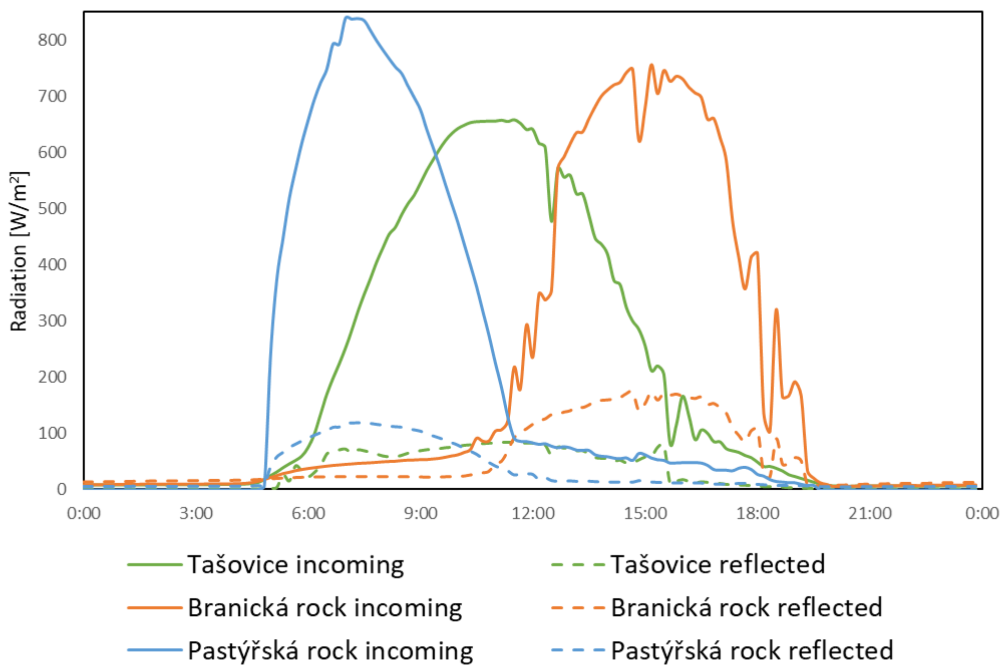

Figure 5: Example of the incoming and reflected radiation measured by pyranometers at Branická rockS, Tašovice and Pastářská rockS sites. 24-hour time series of incoming and reflected radiation. Data were recorded 1.8.2020 with no clouds. Influence of slope aspect is obvious from peak incoming radiation shift.

5.3 Borehole temperature

By continuous temperature measuring in different depths inside a sub-horizontal borehole, we can observe both diurnal and annual temperature amplitude in various depths (Fig. 65). In-depth measurements of temperature show differences in temporal thermal behaviour between monitored rock slopes (Fig. 56,7). From boxplots that represents data from all monitored sites (Fig 7.), it is visible that largest surface temperature variation has been measured at Tašovice site..~~it is obvious that largest surface temperature variation has been measured at Tašovice site despite the shortest operating time.~~ This is probably caused by the dark colour of Tašovice rock surface, with lower albedo. However, in greater depths, this variation decreases. This is probably caused by lower thermal diffusivity of the granite. Moreover, in the depth of the rock mass the influence of direct sunlight is attenuated. ~~This is probably caused by the dark colour of Tašovice rock surface, with lower albedo.~~ Greater in-depth temperature variation is present at Pastýřská rock site. However, these data can be biased by different time-series lengths (1 vs 2 full years). Effect of different aspect is visible from peak of diurnal temperature, when on east facing rock slope (Pastýřská rock) temperature peaks earlier then on SSE facing Tašovice and WSW facing Branická rock (Fig. 6). Differences in lithology (different thermal diffusivity) causes temporal shift between surface and subsurface temperature peaks. This temporal shift differs between the different rock slopes. Higher median of the in-depth temperature at Pastýřská and Branická rocks (Fig. 7) is caused by longer in-depth temperature time-series, spanning over two summer periods (Fig. 6).~~Overall differences caused mainly by lithology and aspect are visible.~~

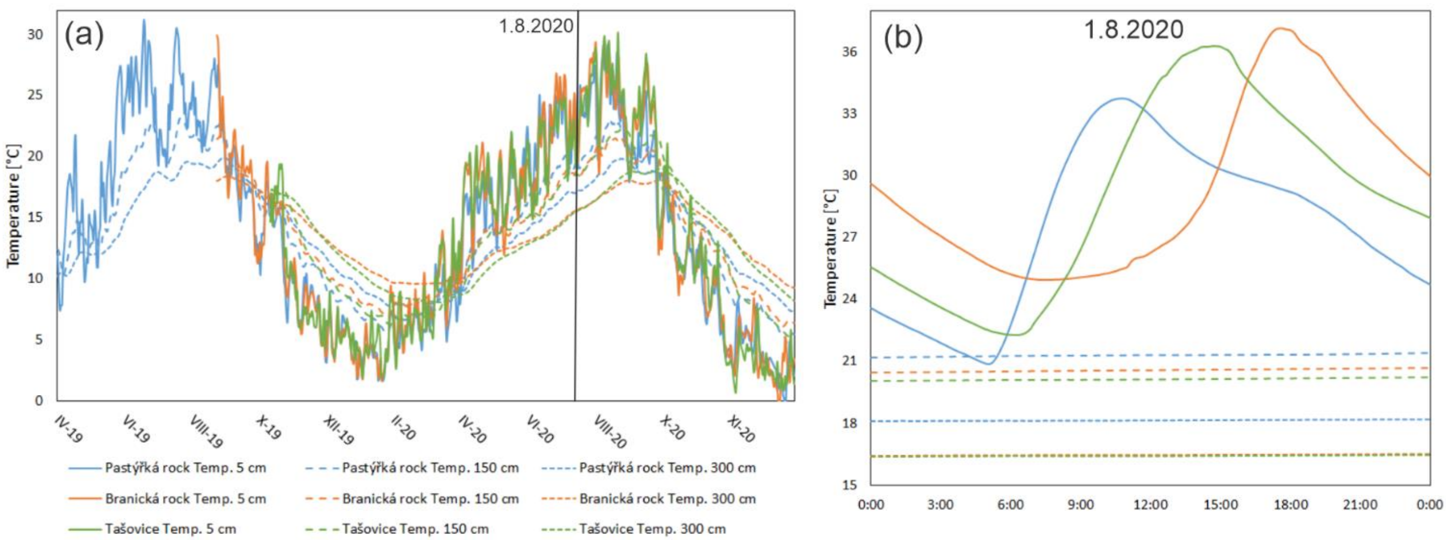

Figure ~~5~~6: Comparison of temperatures in different rock slope depths (5, 150 and 300 cm) at three monitored rock slopes. (a): long-term data (daily average), (b): one day data from 1.8. 2020

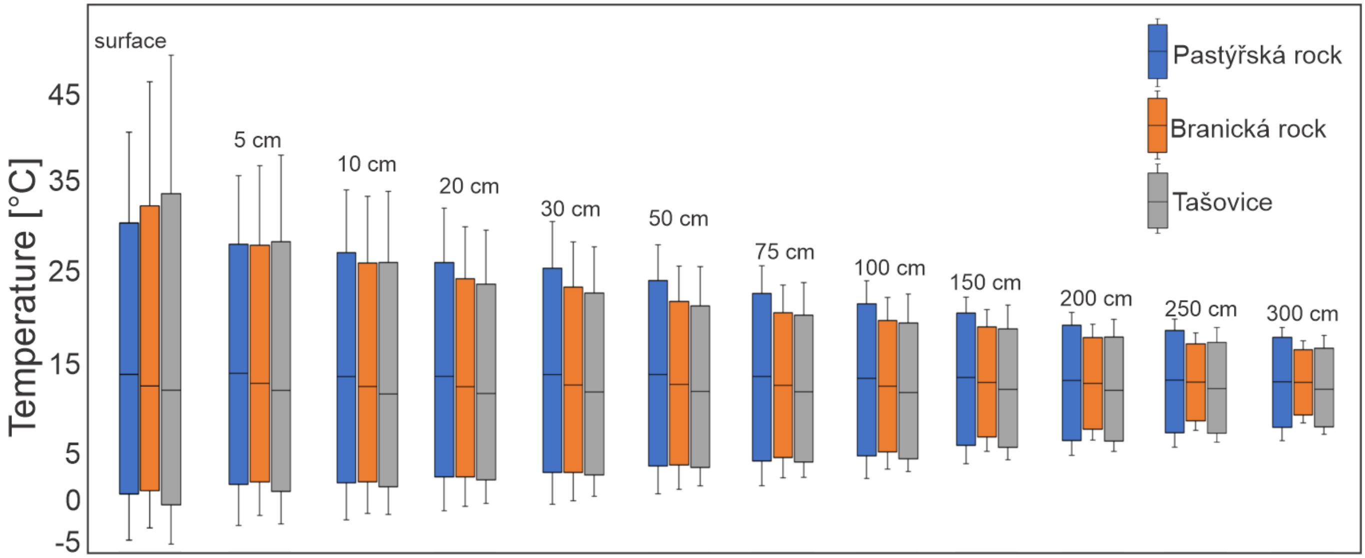

Figure ~~7~~6: ~~Comparison of in – depth rock mass temperature data from all three monitored sites.~~ Comparison of in – depth rock mass temperature data from all three monitored sites. Boxplots shows median, minimum, maximum, first and third quartile of temperature data.

5.4 Blocks dilatation

At all monitored sites, ~~we are observing~~ the thermally-induced dilatation of individual blocks is observed.~~,~~ ~~h~~However, due to relatively short time-series, the measured crack movements do not yet show ~~significant opening or closing~~ any irreversible trends~~ yet~~ unrelated to air temperature visible on graphs. From the ~~measured dilatation~~ crackmeters data, diurnal and annual amplitudes of crack opening ~~for each instrumented block~~ can be identified for all monitored rock blocks. Fig. ~~7~~ 9 shows measured diurnal and annual rock ~~block dilatation~~crack opening at Pastýřská rock site. From the ~~figure~~ graph it is visible the influence of diurnal and annual temperature changes on the crackmeter position ~~opening~~. Similar behaviour is observed within ~~on~~ all monitored blocks ~~(Table 6)~~.

The amplitude of crack meters position differs between individual sites and blocks (Table 6, Fig. 8). These differences are caused by different blocks dimensions, time series length, crack~~-~~meters placement and the regime of destabilization.

Site	Block	Crack meter position amplitude Δ l [mm]				measuring since
		CM1-P1	CM1-P2	CM2-P1	CM2-P2	
Pastýřská rock	1	1.05	0.95	0.75	0.75	23.10.18
Branická rock	1	1.45	0.35	0.25	N/A	4.6.19
	2	0.4	0.5	N/A	N/A	20.6.19
	3	0.75	0.7	N/A	N/A	10.7.20
Tašovice	1	0.65	0.25	N/A	N/A	4.12.18
	2	0.6	0.75	N/A	N/A	4.12.18
	3	0.85	0.7	N/A	N/A	18.10.19

Table 6: Amplitude of crack meters measuring at Pastýřská rock: 1 block 4 crack meters, Branická rock: 3 blocks 7 crack meters and Tašovice: 3 blocks 6 crack meters. The table shows the difference between maximal and minimal opening of all placed crack meters. CM: crackmeter, P: position Last measured data: 27.1.2021~~**Table 6: Amplitude of crack meter measuring at Pastýřká rock: 1 block 4 crack meters, Branická rock: 3 blocks 7 crack meters and Tašovice: 3 blocks 6 crack meters. The table shows the difference between maximal and minimal opening of all placed crack meters. Last measured data: 27.1.2021**~~

So far, crack meter amplitudes (Fig. 8, Table 6) higher than 1 mm ~~, relatively high crack meter amplitudes~~ were measured on Block 1 (aprox. 170 m^3) at Pastýřská rock site (PR1_1, PR1_2) and on Block 1 (aprox. 16 m^3) at Branická rock site (BR1_1, BR1_2, BR2_1). These blocks are the two largest ~~ones~~ instrumented. ~~Measured crack meter amplitude is caused by block thermal expansion/contraction~~ Measured crack meter amplitude is reversible and thus caused by block thermal expansion/contraction. ~~On the other hand, r~~Relatively small block 3 at Branická rock site (BR4_1,BR4_2) shows movements larger than 0.5 mm although is instrumented only since summer 2020.~~(BS site) shows relatively large movements although is instrumented only since summer 2020~~. ~~These movements points on possible gradual destabilization of this block.~~ Such a large amplitude suggests that the block is unstable and by further monitoring this hypothesis should be confirmed.

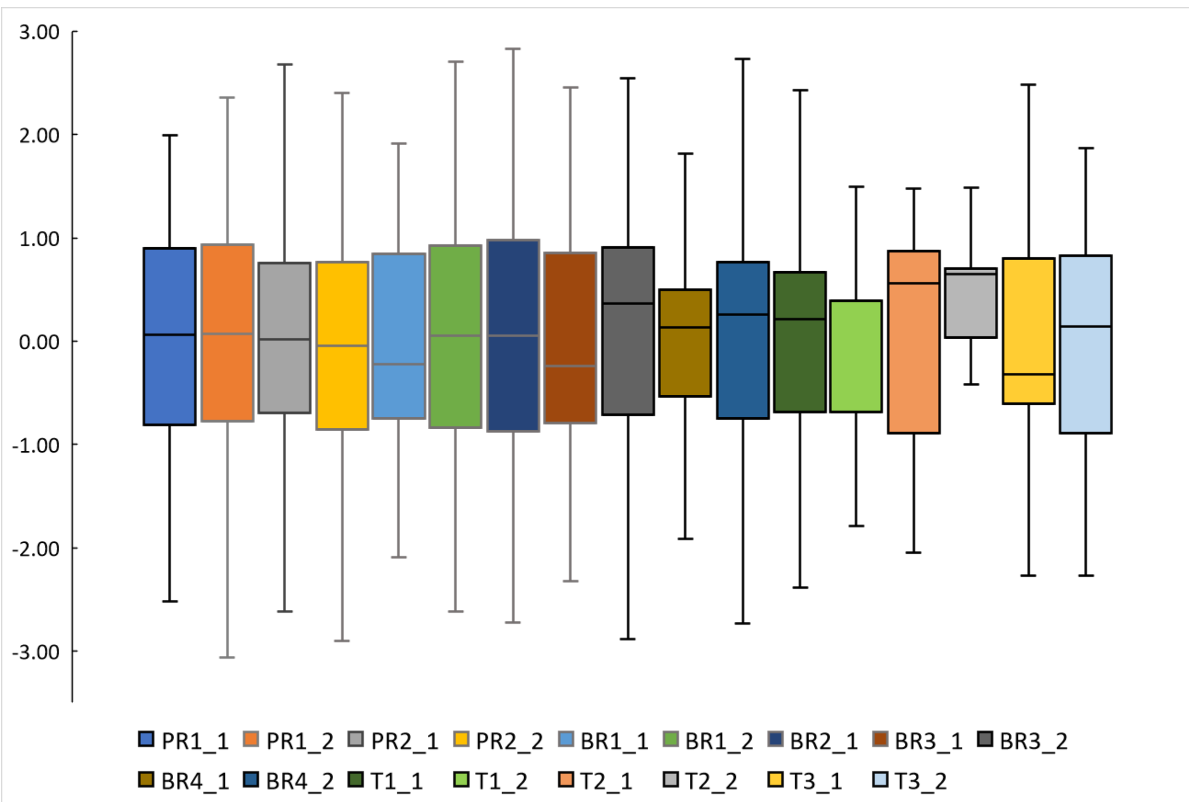

Figure 8: Box plots of crackmeters positions data. To comparison of different positions of measurements, data were standardised. Boxplots shows max/min of crack meter position, median, first and third quartile.

Blocks that are instrumented at Tašovice site seems to be more stable (Table 6, Fig. 8). Only Block 3 shows 0.85 mm of reversible movement. Again, this block was instrumented ~~recently~~ at the end of 2019. By further monitoring~~,~~ analyses of crackmeter position graphs and statistical trend analyses possible blocks´ irreversible temperature unrelated trends should be revealed. ~~trend analyses should reveal possible blocks´ destabilization trends. Larger blocks (PS1, BS1; BS2) shows the largest overall amplitude of movements. Rest of smaller blocks shows smaller overall amplitudes, however these seams to be more influenced by the short-term diurnal temperature changes. Sensitivity to fast heating/cooling, makes these blocks more susceptible to temperature-induced irreversible movements.~~ Destabilization of the single blocks should be visible as irregularities in crackmeter position time-series not strictly related to thermal dilatation. From Table 7. it is visible that two crackmeters at Tašovice site show large amplitude of movement (T2_2, T3_2), however, these movements shown them self's as fully reversible and really short lasting (one-hour measurement). These were probably caused by external forces, such as weight of snow cover deforming crackmeter body or deformation of anchoring point during maintanence. Larger blocks (PR1, BR1; BR2) shows the largest overall amplitude of movements. Rest of smaller blocks shows smaller overall amplitudes however these seem to be more influenced by the short-term diurnal temperature changes. Sensitivity to fast heating/cooling makes these blocks more susceptible to temperature-induced irreversible movements. When data from all crackmeters are standardized (Fig. 8), largest relative dynamic is visible at Pastýřská rock (PR) and Branická rock (BR) blocks. These crackmeters are placed on the two largest monitored blocks. At Tašovice site, dynamic of crackmeters displacement is generally lower.

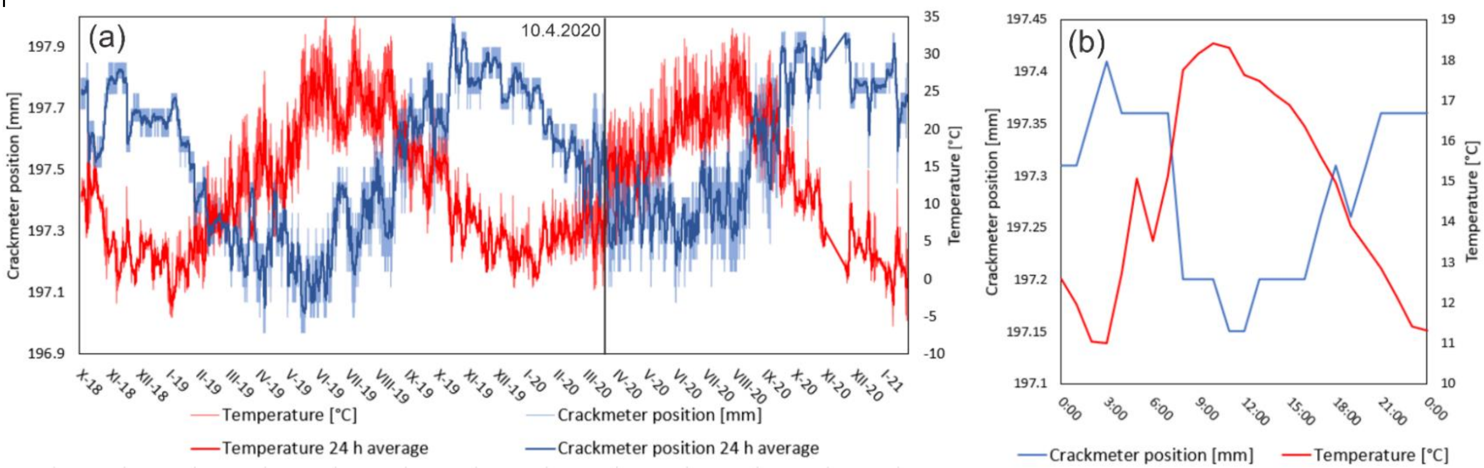

Figure 7: Measured in situ temperature and crack opening at Pastýřská rock site. (a): whole time-series with annual amplitude, (b): example of diurnal amplitude measured on 10.4.2020

6 Discussion

Commonly used rock stability monitoring systems are often designed to provide an early warning (Jaboyedoff et al. 2011; Crosta et al. 2017), aiming primarily at the identification of a hazard and not to investigate the causes or thresholds of the movement acceleration. The presented ~~complex~~ monitoring system is designed to contribute to explaining the various meteorological and temperature related influences on the destabilizing processes, which leads to the eventual loss of rock mass stability and rock fall event triggering (Viles, 2013). Fantini et al. (2017) have concluded that it is the temperature variations (rather than precipitation or wind) that cause changes in internal strain within the rock mass leading to its destabilization. Other factors, such as climate change, former rock fall, seismic stress or hydrological processes are more responsible for rock fall triggering than for short-term strain field modification (Krautblatter and Moser 2009). However, to assess the strain changes within the rock mass, it is necessary to have information on the temperature distribution inside the rock slope depth. This is the crucial advantage of the presented monitoring system, as the borehole temperature ~~monitoring~~ compound probe allows to identify short and long-term temperature changes up to 3 m depth.

To observe individual thermally-induced influences of the strain in the rock masses related to air, rock mass temperature and solar radiation, we have placed the monitoring system on rock slopes with various aspect (different insolation and its diurnal and annual changes) and built of different rocks (sandstone, granite and limestone) to include the influence of heat conductivity, capacity and colour of the rock. While there are numerous laboratory studies on rock conductivity (cf. Blásquez et al. 2017), modelling of heat flow based on surface observation (Hall and André, 2001, Marmoni et al. 2020), ~~or coarse,~~ large-scale experiments usually aiming at heat management in the thermal energy industry (Zhang et al. 2018), only a few experiments have been carried concerning the shallow (first meters)~~, first meters surface of the rocks~~ subsurface zone of rock slope ~~-~~(Greif et al. 2017, Magnin et al. 2015a), even though this is the most strained and weathered part of the natural rock mass (Marmoni et al. 2020). Moreover, thermal conductivity or rock strength can be spatially determined from heating/cooling rates of rock slope surface using thermal camera (Pappalardo et al. 2016; Pappalardo and D'Olivo, 2019; Fiorucci et al. 2018; Guerin et al. 2019). Our approach is aiming to combine these methods, to create simplified numerical thermomechanical models of monitored rock slopes/partial unstable blocks.

The analyses of structural properties of rock were performed using traditional field compass measurements and ~~using~~ automatic discontinuity extraction from the UAV SfM photogrammetry produced point clouds using DSE software (Riquelme et al., 2014).~~from the point clouds.~~ While generally, the results were similar, the point cloud analysis ~~does~~ did not include discontinuity sets that are not forming the surface of the rock face. This effect is visible mainly in the case of the Tašovice rock slope 3D model, where the structural setting is not so straight forward as it is at Branická rock and Pastýřská rock sites formed by sedimentary layers.

Concerning the proposed monitoring system, it is compact, built of cheap and easily accessible off-the-shelf components (Tables 1 and 2), and easy to modify according to specific conditions at rock the slope site. The performance of the monitoring system was so far without major problems. One crack meter datalogger was damaged and one pyranometer was destroyed by a rockfall triggered by a severe thunderstorm. Otherwise, monitoring works reliably at all instrumented sites. Maintenance is consisting of changing datalogger batteries and cleaning rain gauge buckets. Online data transfer via Sigfox IoT network (dilatometers) and GSM (~~environmental~~ weather stations) works without problems.

A disadvantage of crackmeter use is that this method provides only one-dimensional spatial change data. On the other hand, this instrumentation is relatively affordable, with good one-dimensional precision and temporal resolution (Table 2). This allows to place multiple crackmeters within one instrumented site. To get full 3D data about an unstable feature´s spatio-temporal behaviour, more crackmeters must be deployed. Additionally, 3D data about larger spatial changes within rock slopes are acquired by UAV SfM photogrammetry and TLS campaigns.

~~Crack meters can record movements smaller than 0.1 mm (Tables 1,7). In comparison with other methods that measure spatial change, their precision is high, with lower costs (Table 7). The temporal resolution of the measurement is nearly continuous when the crack meter position can be read every second (Table 7). Moreover, we have tested these in a controlled temperature environment using a climate chamber to find out any temperature-dependent errors. In this controlled test, we were able to measure the expansion of a concrete block. The resulting block expansion measurements matched theoretically calculated concrete block expansion. This way we made sure, that measurement of the crack meters is not biased by dilatation of the device itself. A disadvantage of crack meter use is that this method provides only one-dimensional spatial change data. To get full 3D data about an unstable feature´s spatio-temporal behaviour, more crack meters must be deployed. Also, the maximum range of this device is limited to 200 mm. That limits the use of this crack meters to changes with lower magnitude.~~

Crack meter	PR1_1	PR1_2	PR2_1	PR2_2	BR1_1	BR1_2	BR2_1	BR3_1	BR3_2	BR4_1	BR4_2	T1_1	T1_2	T2_1	T2_2	T3_1	T3_2
Mean	197.55	99.18	100.36	57.34	109.10	131.13	108.21	80.77	21.56	53.61	73.23	62.64	90.53	130.65	125.39	115.86	112.41
Variance	0.05	0.03	0.02	0.01	0.14	0.00	0.00	0.01	0.01	0.02	0.01	0.01	0.00	0.03	0.76	0.03	0.02
Stdev	0.23	0.17	0.13	0.12	0.38	0.06	0.06	0.10	0.09	0.14	0.10	0.11	0.04	0.16	0.87	0.17	0.14
Median	197.56	99.19	100.36	57.34	109.06	131.14	108.23	80.78	21.59	53.63	73.26	62.66	90.55	130.74	125.96	115.80	112.43
Q3	197.75	99.34	100.46	57.44	109.50	131.14	108.28	80.83	21.64	53.68	73.31	62.71	90.55	130.79	126.01	116.00	112.53
Q1	197.36	99.05	100.27	57.24	108.77	131.09	108.18	80.68	21.49	53.53	73.16	62.56	90.50	130.50	125.42	115.75	112.28
Min	196.95	98.60	100.02	56.90	108.28	130.94	108.03	80.54	21.29	53.14	72.92	62.27	90.40	130.31	122.64	115.46	107.45
Max	198.00	99.59	100.75	57.63	109.74	131.33	108.38	80.98	21.78	53.97	73.60	63.10	90.70	130.89	126.69	116.29	112.67

~~**Table 8: Basic statistical descriptions of data measured by all 17 installed crack meters. PR: Pastýřská rock, BR: Branická rock, T: Tašovice**~~

In the case of environmental monitoring, we have found differences between sites (Table 5~~4~~), caused by aspect and local microclimate. Some differences between sites are caused by different length of meteorological variables time-series (Table ~~4~~5). When temperature data from in-depth borehole compound probe ~~monitoring~~ are compared, differences between monitored sites are apparent (~~Figures~~ Fig. 6~~5~~,7~~6~~)~~.,~~ B~~b~~oth diurnal (cca 150 cm depth) and annual temperature cycles (up to 3 m depth)~~, and as deep as 3 m.~~ for each site can be defined. ~~These d~~Differences between these are caused by the combination of the different ~~orientation~~ aspect of rock slopes and by the thermal behaviour of the different rock types. In further continuation of research, spatial data about rock slope surface temperature will be gained using time lapse thermal camera sensing (Racek et al., 2021). As concerns the weather station and borehole compound temperature probe energy supply, the solar panel is capable of keeping the battery charged even during cloudy weather or snowy winters.

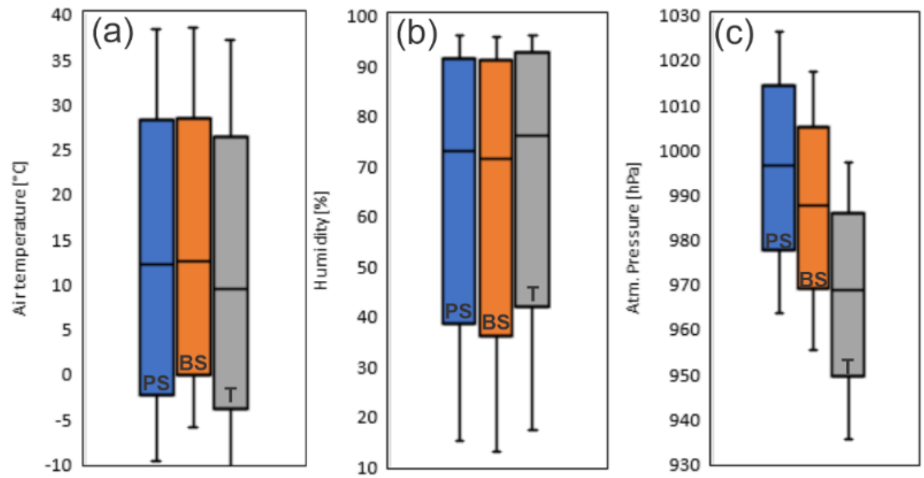

~~**Figure 8: Comparison of air temperature (a), humidity (b) and air pressure (c) data sets, between Pastýřská rock (PS), Branická rock (BS) and Tašovice (T) sites.**~~

Solar radiation balance is not directly comparable, due to different aspect and slope of ~~monitored~~ instrumented rock slabs. However, the temporal shift in maximum radiance caused by general rock slope aspect is visible from resulted solar radiation data (Fig. 54). When ~~whole year~~complete annual data about solar radiance will be available in summer 2021, more differences should be found. Then the comparison of long-term solar radiation cycles and theirs influence on rock slope dynamic will be possible.

	T Air [°C]			1 h. prec. [mm]			Humidity [%]			Air pressure			T rock face [°C]			T 5 cm [°C]			T 10 cm [°C]			T 20 cm [°C]		
	PR	BR	T	PR	BR	T	PR	BR	T	PR	BR	T	PR	BR	T	PR	BR	T	PR	BR	T	PR	BR	T
Mean	12.1	12.4	9.4	0.1	0.1	0.0	72.9	71.2	75.8	996.4	987.4	968.5	14.6	13.3	12.8	14.5	13.4	12.6	14.6	13.5	12.7	14.7	13.5	12.7
Variance	72.0	71.5	71.6	0.3	0.5	0.1	301.6	324.9	305.1	75.2	72.8	79.0	79.6	80.9	98.3	67.9	65.9	72.9	65.4	61.7	65.3	61.1	55.6	57.8
Stdev	8.5	8.5	8.5	0.5	0.7	0.2	17.4	18.0	17.5	8.7	8.5	8.9	8.9	9.0	9.9	8.2	8.1	8.5	8.1	7.9	8.1	7.8	7.5	7.6
Median	11.4	11.9	8.2	0.0	0.0	0.0	78.8	76.6	82.6	996.6	987.7	968.9	14.1	11.7	10.5	14.5	12.3	11.0	14.7	12.5	11.3	14.9	12.8	11.6
Q_3	18.3	18.5	15.5	0.0	0.0	0.0	86.8	86.1	89.3	1002.0	992.9	974.3	21.3	19.4	19.2	21.1	19.8	19.4	21.3	19.8	19.4	21.3	19.7	19.0
Q_1	4.9	5.5	2.4	0.0	0.0	0.0	61.6	58.9	66.5	991.3	982.7	963.3	6.5	5.8	4.5	6.8	6.3	5.2	7.0	6.5	5.4	7.2	6.7	5.7
Min	-9.8	-5.9	-10.4	0.0	0.0	0.0	15.1	12.9	17.4	963.6	955.3	935.5	-3.7	-2.4	-4.2	-2.1	-1.1	-2.0	-1.3	-0.6	-0.7	-0.3	0.1	0.5
Max	38.2	38.4	37.0	28.6	36.5	18.8	96.1	95.8	96.1	1026.3	1017.2	997.1	41.3	46.9	49.8	36.2	37.2	38.4	35.4	34.6	35.2	33.5	31.4	31.0

	T 30 cm [°C]			T 50 cm [°C]			T 75 cm [°C]			T 100 cm [°C]			T 150 cm [°C]			T 200 cm [°C]			T 250 cm [°C]			T 300 cm [°C]		
	PR	BR	T	PR	BR	T	PR	BR	T	PR	BR	T	PR	BR	T	PR	BR	T	PR	BR	T	PR	BR	T
Mean	14.7	13.5	12.7	14.6	13.5	12.8	14.5	13.5	12.8	14.4	13.6	12.9	14.3	13.7	13.0	14.1	13.8	13.0	14.0	13.8	13.1	13.9	13.8	13.1
Variance	56.8	50.4	52.9	49.7	41.9	46.0	43.3	34.4	39.4	37.7	29.0	34.4	29.2	21.0	26.3	23.3	15.2	20.2	19.0	11.4	15.7	15.6	8.6	12.3
Stdev	7.5	7.1	7.3	7.0	6.5	6.8	6.6	5.9	6.3	6.1	5.4	5.9	5.4	4.6	5.1	4.8	3.9	4.5	4.4	3.4	4.0	3.9	2.9	3.5
Median	15.1	13.0	11.9	15.1	13.4	12.4	14.9	13.7	12.9	14.7	13.7	13.2	14.2	14.0	13.0	13.8	13.7	13.0	13.9	13.7	12.9	13.8	13.7	12.9
Q_3	21.2	19.3	18.5	21.0	18.8	17.9	20.6	18.6	17.6	20.2	18.3	17.4	19.6	18.0	17.0	18.8	17.4	16.9	18.2	16.8	16.5	17.7	16.5	16.2
Q_1	7.4	7.0	6.0	7.6	7.4	6.4	7.8	7.8	6.7	8.2	8.2	6.9	8.8	9.3	7.9	9.2	9.9	8.6	9.8	10.6	9.2	10.3	11.1	9.8
Min	0.3	0.7	1.3	1.5	2.0	2.3	2.4	3.3	3.3	3.3	4.3	4.0	4.7	6.1	5.2	5.8	7.5	6.2	6.6	8.5	7.2	7.4	9.4	8.1
Max	31.6	29.3	28.8	28.9	26.6	26.5	26.8	24.6	24.9	25.4	23.5	23.9	23.2	21.8	22.3	21.7	20.3	20.9	20.7	19.2	19.8	19.9	18.4	19.0

~~**Table 9: Basic statistical descriptions of atmospheric and borehole temperature monitoring.**~~

It is necessary to remark that the destabilisation processes are rather slow and have a low magnitude in the central European mid-latitude climate because of lower temperature amplitude, shorter period of active freeze thaw cycles or lower amount of precipitation (Krautblatter and Moore, 2014; Hermans and Longva, 2012; Viles, 2013).. Therefore, long-term time series monitoring is necessary. In addition to these complications, we are preparing installation of monitoring system installation in the Krkonoše Mountains (northern Czechia) at the altitude of 1270 m a.s.l. . In this mountainous environment, block destabilization processes act with greater intensity. Also, there are several cycles with different length, amplitude and depth-reach, ranging from diurnal cycles up to long-term cycles linked with solar activity or climatic oscillations (Gunzburger et al. 2005; Sass and Oberlechner., 2012; Pratt et al. 2019). Among these are the most prominent diurnal and annual cycles (Marmoni et al. 2020). Diurnal cycles have shallower reach (see Fig. 56), but are fast and thus cause high intensive strain in the surficial rock layer., while aAnnual cycles are slower, but with higher amplitudes and depth reach (Hall and André, 2001). This informationIn depth temperature data will helps to clarify the role of thermally-induced stress in rock disintegration. Temperature changes causes irregular heating and cooling of rock mass. These leads to irregularities in rock mass dilatation at surface and in depth, which causes thermally induced stress/strain, which eventually can lead to discontinuity evolution and breakage of rock mass surface layers. Thermally-driven disintegration also acts at grain scale where grains of different minerals expand differently and induce stresses in to rock mass (Hall and André, 2001,2003).

Also, iIn combination with the temperature and global solar radiation measurements, heat conduction velocity inside of rock mass can be determined. Diurnal temperature cycles with higher magnitude can play a crucial role in rock fall triggering (Gunzburger et al. 2005; Collins and Stock, 2016). This, together with mechanical properties of the rock mass (Table 23), will allow creating more accurate thermomechanical models of the monitored rocks slopes in the future. These models , complemented with information on the structural data, mechanical properties of rock mass, IR camera surface temperature and radiation balance of surface measured with pyranometers will help to identify zones where the accumulation of thermally-induced stress concentratesbe used to identify zones where the accumulation of thermally induced stress concentrates, as the places of potential failure and following destabilization of the rock slopedestruction and following destabilization of the rock slope. To calibrate and validate the numerically simulated thermal conductivity, timeseries of in-depth rock mass temperature will be used. Numerical models of partial monitored blocks dilatation and thermally induced stress field changes will follow.

On all sites, the highest diurnal measured crack meter movements are recorded in the spring and autumn months, when diurnal rock slope surface temperature changes have the largest magnitude. These conditions when the temperature at night falls 0°C and during daytime again rises, are crucial to freeze-thaw cycles development and consequent destabilization of the rocks. We are expecting that irreversible crackmeter position trends will accumulate during these periods.

Several works that use similar monitoring instrumentation and approaches were published In other works that using similar instrumentation was published in past. (Matsuoka 2008; Bakun-Mazor et al. 2013,2020; Dreabing, 2020; Draebing et al. 2017 Nishi and Matsuaoka 2010)., Despite that,although in thermally induced rock mass deformations monitoring is still relatively marginally studied field. Matsuoka (2008) presented long-term data of crack meter monitoring. His data were collected on rock slopes in high mountainous alpine environment.rock slope unstable parts in alpine environment. Similarly, to our results joint dynamic presented by Matsuoka (2008) is influenced by in-situ air and rock mass temperature. ~~Same as in our results, measured joint dynamic is influenced by air and rock mass temperature. Similarly, to our first data,~~Measured dynamic of monitored joints is highest in spring and autumn, which also corresponds with ours results.~~.~~ ~~Because longer time span of monitoring~~ From relatively long crackmeter timeseries Matsuoka (2008) ~~measured~~ defined gradual, temperature-driven joint opening. Most significant Most significant changes in crack meter position are explained by freeze-thaw conditions. ~~joint opening is in his work linked with freeze-thaw conditions in alpine environment.~~ Nevertheless, even in dynamic alpine environment, joint opening is slow, spanning approx. 0.4 mm in ~~2~~ two years of continuous monitoring. ~~Is~~ It is expected, that in temperate climate these processes are even slower. Nishi and Matsuaoka (2008) ~~presented~~ described influence of temperature to large rock slide temporal displacement. In this, to our sites different destabilization mode and mechanism~~setup~~, they have measured large displacement over ~~1 m~~one meter in ~~3~~ three years of monitoring. Movement accelerations were documented during highest precipitations periods.~~Largest movements velocities were documented during highest precipitations seasons.~~ Due to different structural setting and spatial scale of monitored rock slope parts~~spatial extent of monitored rock mass~~ ~~movements are~~ these results ~~almost~~ are incomparable. Bakun-Mazor et al. (2013, 2020) proposed monitoring system to distinguish thermally and seismically induced joint movements in limestone and dolomites a Masada cultural heritage site. Measured amplitude of thermally-induced irreversible joint movements reached approx. 0.3 mm in one year. With these data, they have described concept of thermally-driven wedging-ratcheting mechanism. Estimated annual irreversible joint opening at Masada was approx. 0.2 mm. In this study, thermally-induced irreversible movements are combined with seismically-induced movements that have higher magnitude.~~In this work amplitude of thermally induced joint movements was approximately 0.3 mm in one year. Which is similar to our first results. In this work, they have estimated annually irreversible joint opening about 0.2 mm. However, in this study, thermally induced movements are supplemented with seismically induced movements with higher magnitude.~~

We ~~hope~~assume, that in long-term (several years), we will be able to observe similar wedging-ratcheting mechanism with lower amplitude at our sites. During colder periods, this mechanism can be supported with frost shattering.~~, where also effect of frost shattering should play not negligible role.~~

Draebing et al. (2017) and Draebing (2020) ~~observed~~ monitored crack opening in alpine environment. In this extreme environment, they were ~~able to observe~~ observed ~~short-term~~ ice wedging ~~induced~~ driven ~~movements~~ crack opening up to 1 mm in several days doring snowmelt period. ~~These movements were active in snowmelt season, when ice wedging is most active.~~ By comparing in situ crack meter temperature and crack meter opening they have established linkage between in situ temperature and joint dynamic. In ~~this case~~their paper joint dynamic ~~was~~ is also influenced by snow cover.~~, which has in alpine region longer time span than in case of our monitoring sites.~~ Measured gradual irreversible joint opening is approx. 0.1 mm/year. ~~However, even in these conditions, gradual irreversible joint opening is relatively slow, about 0.1 mm/year.~~ Our data from 2020/21 winter period and from newly instrumented site at Krkonoše mointains should show similar results. However, with lack of active permafrost and permanently ice-filled joints at our sites, these movements should have lower magnitude.~~We hope, that data from winter 2020/21 bring similar results in case of our monitoring, however with lack of active permafrost~~

~~and ice filled joints at our sites, these moments should have lower magnitude. Newly instrumented site in Krkonoše mountins should provide data from dynamic mountainous region.~~

Measuring temperature of dry unfrozen rock mass depth is still rarely used approach.~~Measuring temperature inside rock mass is nowadays relatively uncommon technique.~~ measured in depth rock mass temperatures in surface permafrost rock mass zone ~~Only few works estimate in depth rock mass temperatures in surface zone~~ (Magnin et al. 2015a; Fantini et al. 2018). ~~In work of~~ Magnin et al. (2015a) ~~is measured~~measure rock mass temperature inside 10 m deep boreholes. This research is oriented mainly to active permafrost depth estimation and its spatio-temporal behaviour. In shallow subsurface zone, they have measured annual temperature amplitude approx. 5°C in 3 m depth. Our data from sub-horizontal boreholes show rock mass temperature amplitude of approx. 10°C in the depth of 3 m. This is probably caused by different climatic setup of ours sites.~~Boreholes were drilled in alpine, permafrost active areas and this research is oriented mainly to estimate active permafrost depth ant its temporal evolution. In shallow surface zone, they have recorded annual temperature differences approx. 5°C in 3 m depth. Temperature amplitude is rising in shallower subsurface zones. Our data from horizontal boreholes shows amplitude in 3 m approx. 10° C. This is caused by warmer climate and absence of long-term snow cover on rock face.~~

Fantini et al. (2018) studied short-term temperature profiles ~~in~~ at experimental limestone quarry rock slope. Diurnal temperature cycles in their case reached maximum depth of approx. 20-30 cm. These results correspond with our measurements.~~,~~ ~~where w~~We are able to observe diurnal temperature cycles up to 50 cm depth~~,~~ during summer perriod, when rock mass surface is intensively heated by solar radiation. It is necessary to mention, that comparison of these results is not straight forward due to diverse climatic setup.~~Is necessary to mention, that is not easy to compare results, with these works, due to different climatic setup.~~

Currently, the three sites are continuously measuring for a period between 1 and 2 years (Table 5~~4~~). Based on this, we can show that the system is capable of observing the influence of thermal stress to the response of the monitored blocks ~~on the thermal dilatation~~ (Fig. 9~~6~~). However, to exclude seasonality, the time-series of the ~~crack opening~~crackmeters positions should be longer than 2-3 years. In a longer period, we expect to observe the process of long-term rock slope destabilization represented by a gradual irreversible trend of crack opening/closure, which points on to the partial block destabilization. Longer time series also allow~~s users~~ to use~~observe~~ seasonal statistical trend tests to describe trends in monitored joints dynamic.~~the influence of meteorological variables on the rock blocks stability.~~ The influence of meteorological variables on the rock blocks stability will be statistically analysed, to find out how individual meteorological variables influence dynamic of joints. In-depth temperatures will be analysed to find differences in thermal conductivity, diffusivity and seasonal temperature trend between the monitored sites. Differences in thermo-mechanical behaviour of different rock slopes will be studied using numerical modelling. Furthermore, monitoring system will be continuously upgraded. Installation of in-situ strain gauges monitoring is planned to directly observe changes in rock mass surface strain.

7. Conclusions

A newly designed ~~complex~~ rock slope stability monitoring system was introduced. The presented ~~complex~~ monitoring system combines monitoring of meteorological variables with 3 m deep in-rock thermal profile and dilatation of the unstable rock block joints. It brings a unique opportunity to observe long-term gradual changes within the rock ~~mass~~face, ~~destabilizing~~ leading to the rock slope destabilization.

The design of the system allows an easy installation at various locations without major adjustments or changes. All components of the system are available off-the-shelf, at a relatively low price and are easy to replace with low skill requirements. The environmental data are transferred via GSM to a remote server, and the dilatation data are sent via IoT SigFox network or can be downloaded remotely from several tens of meters. Thus, the maintenance visits of the sites can be limited to several months' interval.

The monitored sites are easily comparable as ~~similar~~ identical monitoring set-up and equipment is used. Thus, we are monitoring the reaction of various rock types on a certain climatic event and observing the differences and similarities on particular sites. This concerns not only movements or expansion of the rock mass but also the heat advance into the rock, its velocity and amplitudes, otherwise very difficult to measure. Significant differences in shallow surface rock mass zone are observable from 3 m borehole ~~thermometer~~ thermocouple probe data.

Further development of this project should include the installation of in-situ rock surface ~~stress~~ strain monitoring using in situ placed strain gauges. In following research, in situ gained data will be used for heat flow and heat-induced strain numerical modelling within the rock mass.

Measuring of joint movements combined with temperature and other external influencing factors will be analysed to understand ~~mechanisms~~ contribution of individual processes, leading to rock slope destabilization~~.~~ Whole system will be gradually maintained and placed at more suitable sites. ~~Moreover, it can contribute to explaining the influence of the individual destabilizing processes.~~ ~~Local factors which influence the rock slope stability are described using classical and modern geomorphological, geomechanical or remote sensing methods. Structural and laboratory-measured mechanical rock properties will be used for heat flow and heat-induced strain numerical modelling within the rock mass.~~

8 Acknowledgements

This research was carried out in the framework of the long-term conceptual development research organisation RVO: 67985891, TAČR project number SS02030023 "Rock environment and resources" within program "Environment for life", internal financing from Charles University Progress Q44 and SVV (SVV260438) and the Charles University Grant Agency [GAUK 359421]

References

Bakun Mazor, D., Keissar, Y., Feldheim, A., Detournay, C., Hatzor, Y.H., 2020. Thermally-Induced Wedging–Ratcheting Failure Mechanism in Rock Slopes. Rock Mech Rock Eng 53, 2521-2538.. https://doi.org/10.1007/s00603-020-02075-6

Bakun-Mazor, D., Hatzor, Y.H., Glaser, S.D., Santamarina, J.C., 2013. Thermally vs. seismically induced block displacements in Masada rock slopes. Int J Rock Mech Min (1997) 61, 196-211.. https://doi.org/10.1016/j.ijrmms.2013.03.005

Barton, M.E., McCosker, A.M., 2000. Inclinometer and tiltmeter monitoring of a high chalk cliff, in: Barton, M. E., And A. M. Mccosker. "Inclinometer And Tiltmeter Monitoring Of A High Chalk Cliff." Landslides In Research, Theory And Practice: Proceedings Of The 8Th International Symposium On Landslides Held In Cardiff On 26–30 June 2000. Thomas Telford Publishing, pp. 127-132.

Blikra, L., Christiansen, H.H., 2014. A field-based model of permafrost-controlled rockslide deformation in northern Norway. Geomorphology (Amsterdam) 208, 34-49.. https://doi.org/10.1016/j.geomorph.2013.11.014

Burjanek, J., Gassner-Stamm, G., Poggi, V., Moore, J.R., Faeh, D., 2010. Ambient vibration analysis of an unstable mountain slope. Geophys J Int180, 820-828.. https://doi.org/10.1111/j.1365-246X.2009.04451.x

Burjanek, J., Gischig, V., Moore, J.R., Fah, D., 2018. Ambient vibration characterization and monitoring of a rock slope close to collapse. Geophys J Int212, 297-310.. https://doi.org/10.1093/gji/ggx424

Carla, T., Farina, P., Intrieri, E., Botsialas, K., Casagli, N., 2017. On the monitoring and early-warning of brittle slope failures in hard rock masses: Examples from an open-pit mine. Eng Geol 228, 71-81.. https://doi.org/10.1016/j.enggeo.2017.08.007

Coccia, S., Kinscher, J., Vallet, A., 2016. Microseismic and meteorological monitoring of Séchili-enne (French Alps) rock slope destabilisatio, in: 3. International Symposium Rock Slope Stability (Rss2016), Nov 2016, Lyon, France.. pp. 31-32.

Collins, B.D., Stock, G.M., Eppes, M.C., 2017. Progressive Thermally Induced Fracture of an Exfoliation Dome: Twain Harte, California, USA, in: Isrm Progressive Rock Failure Conference, 5-9 June, Ascona, Switzerland.

Collins, B., Stock, G.M., 2016. Rockfall triggering by cyclic thermal stressing of exfoliation fractures. Nat Geosci9, 395-400.. https://doi.org/10.1038/ngeo2686

Crosta, G.B., Agliardi, F., Rivolta, C., Alberti, S., Dei Cas, L., 2017. Long-term evolution and early warning strategies for complex rockslides by real-time monitoring. Landslides 14, 1615-1632.. https://doi.org/10.1007/s10346-017-0817-8

D'Amato, J., Hantz, D., Guerin, A., Jaboyedoff, M., Baillet, L., Mariscal, A.M., 2016. Influence of meteorological factors on rockfall occurrence in a middle mountain limestone cliff. Nat Hazard Earth Sys 16, 719-735.. https://doi.org/10.5194/nhess-16-719-2016

Dewez, T.J.B., Girardeau-Montaut, D., Allanic, C., Rohmer, J., 2016. Facets: A cloudcompare plugin to extract geological planes from unstructured 3d point clouds, in: Int Arch Photogramm Vol. 41, Iss. B5. Prague, CZECH REPUBLIC, pp. 799-804.

do Amaral Vargas, E., Velloso, R.Q., Chávez, L.E., Gusmao, L., 2013. On the Effect of Thermally Induced Stresses in Failures of Some Rock Slopes in Rio de Janeiro, Brazil. Rock Mech Rock Eng 46, 123-134.. https://doi.org/10.1007/s00603-012-0247-9

Draebing, D., 2020. Identification of rock and fracture kinematics in high Alpine rockwalls under the influence of altitude.. Earth Surf Dynam Discuss 1-31.. https://doi.org/https://doi.org/10.5194/esurf-2020-69

Du, Y., Xie, M.-wen, Jiang, Y.-jing, Li, B., Chicas, S., 2017. Experimental Rock Stability Assessment Using the Frozen–Thawing Test. Rock Mech Rock Eng 50, 1049-1053.. https://doi.org/10.1007/s00603-016-1138-2

Draebing, D., Krautblatter, M., Hoffmann, T., 2017. Thermo-cryogenic controls of fracture kinematics in permafrost rockwalls. Geophys Res Lett 44, 3535-3544.. https://doi.org/10.1002/2016GL072050

Eppes, M., Magi, B., Hallet, B., Delmelle,, E., Mackenzie-Helnwein, P., Warren, K., Swami, S., 2016. Deciphering the role of solar-induced thermal stresses in rock weathering. Geol Soc Am Bull128, 1315-1338.. https://doi.org/10.1130/B31422.1

Fantini, A., Fiorucci, M., Martino, S., Marino, L., Napoli, G., Prestininzi, A., Salvetti, O., Sarandrea, P., Stedile, L., 2016. Multi-sensor system designed for monitoring rock falls: the experimental test-site of Acuto (Italy). Rendiconti Online Societa Geologica Italiana 41, 147-150.. https://doi.org/10.3301/ROL.2016.115

Fiorucci, M., Marmoni, G.M., Martino, S., Mazzanti, P., 2018. Thermal Response of Jointed Rock Masses Inferred from Infrared Thermographic Surveying (Acuto Test-Site, Italy). Sensors 18, 2221.. https://doi.org/10.3390/s18072221

GEFRAN, 2020. Position Transducers, 1st ed. 25050 PROVAGLIO D'ISEO (BS) ITALY.

Girardeau-Montaut, D. (2016). CloudCompare. *Retrieved from CloudCompare: https://www. danielgm. net/cc*.

Girard, L., Beutel, J., Gruber, S., Hunziker, J., Lim, R., Weber, S., 2012. A custom acoustic emission monitoring system for harsh environments: application to freezing-induced damage in alpine rock walls. Geosci Instrum Meth1, 155-167.. https://doi.org/10.5194/gi-1-155-2012

Greif, V., Brcek, M., Vlcko, J., Varilova, Z., Zvelebil, J., 2017. Thermomechanical behavior of Pravcicka Brana Rock Arch (Czech Republic). Landslides 14, 1441-1455.. https://doi.org/10.1007/s10346-016-0784-5

Gruber, S., Hoelzle, M., Haeberli, W., 2004. Permafrost thaw and destabilization of Alpine rock walls in the hot summer of 2003. Geophys Res Lett31.. https://doi.org/10.1029/2004GL020051

Guerin, A., Jaboyedoff, Michel, Collins, Brian D., Derron, Marc-Henri, Stock, Greg M., Matasci, Battista, Boesiger, Martin, Lefeuvre, Caroline, Podladchikov, Yury Y., 2019. Detection of rock bridges by infrared thermal imaging and modeling. Sci Rep-UK9, 13138-13138.. https://doi.org/10.1038/s41598-019-49336-1

Gunzburger, Y., Merrien-Soukatchoff, V., 2011. Near-surface temperatures and heat balance of bare outcrops exposed to solar radiation. Earth Surface Processes and Landforms 36, 1577-1589.. https://doi.org/10.1002/esp.2167

Gunzburger, Y., Merrien-Soukatchoff, V., Guglielmi, Y., 2005. Influence of daily surface temperature fluctuations on rock slope stability: case study of the Rochers de Valabres slope (France). Int J Rock Mech Min (1997) 42, 331-349.. https://doi.org/10.1016/j.ijrmms.2004.11.003

Hellmy, M.A.A., Muhammad, R.F., Shuib, M.K., Fatt, N.T., Abdullah, W.H., Abu Bakar, A., Kugler, R., 2019. Rock Slope Stability Analysis based on Terrestrial LiDAR and Scanline Survey on Karst Hills in Kinta Valley Geopark, Perak, Peninsular Malaysia. Sains Malaysiana 48, 2595-2604.. https://doi.org/10.17576/jsm-2019-4811-29

Hoelzle, M., Azisov, E., Barnadum, M., Huss, M., Farinotti, D., Hagg, W., Kenzhebaev, R., Kronenberg, M., Machguth, H., Merkushin, A., Moldobekov, B., Petrov, M., Saks, T., Salzmann, N., Schone, T., Tarasov, Y., Usubaliev, R., Vorogushyn, S., Yakovlev, A., Zemp, M., 2017. Re-establishing glacier monitoring in Kyrgyzstan and Uzbekistan, Central Asia. Geosci Inst Meth 6, 397-418.. https://doi.org/10.5194/gi-6-397-2017

Chen, T., Deng, J., Sitar, N., Zheng, J., Liu, T., Liu, A., Zheng, L., 2017. Stability investigation and stabilization of a heavily fractured and loosened rock slope during construction of a strategic hydropower station in China. Eng Geol 221, 70-81.. https://doi.org/10.1016/j.enggeo.2017.02.031

Isaka, B.L.A., Gamage, R.P., Rathnaweera, T.D., Perera, M.S.A., Chandrasekharam, D., Kumari, W.G.P., 2018. An Influence of Thermally-Induced Micro-Cracking under Cooling Treatments: Mechanical Characteristics of Australian Granite. Energies 11, 1338.. https://doi.org/10.3390/en11061338

Jaboyedoff, M., Oppikofer, T., Derron, M.H., Blikra, L.H., Böhme, M., Saintot, A., 2011. Complex landslide behaviour and structural control: a three-dimensional conceptual model of Åknes rockslide, Norway. Geological Society, London, Special Publications 351.

Jaboyedoff, M., Ornstein, P., Rouiller, R.D., 2004. Design of a geodetic database and associated tools for monitoring rock-slope movements: the example of the top of Randa rockfall scar. Nat Hazard Earth Sys 4, 187-196.. https://doi.org/10.5194/nhess-4-187-2004

Janeras, M., Jara, J.-A., Royan, M.J., Vilaplana, J.-M., Aguasca, A., Fabregas, X., Gili, J.A., Buxo, P., 2017. Multi-technique approach to rockfall monitoring in the Montserrat massif (Catalonia, NE Spain). Eng Geol 219, 4-20.. https://doi.org/10.1016/j.enggeo.2016.12.010

Kinoshita, N., Yasuhara, H., 2011. Thermally Induced Behavior of the Openings in Rock Mass Affected by High Temperatures. Int J Geomech11, 124-130.. https://doi.org/10.1061/(ASCE)GM.1943-5622.0000063

Klimes, J., Rowberry, M.D., Blahut, J., Briestensky, M., Hartvich, F., Kost'ak, B., Rybar, J., Stemberk, J., Stepancikova, P., 2012. The monitoring of slow-moving landslides and assessment of stabilisation measures using an optical–mechanical crack gauge. Landslides 9, 407-415.. https://doi.org/10.1007/s10346-011-0306-4

Kromer, R., Walton, G., Gray, B., Lato, M., 2019. Development and Optimization of an Automated Fixed-Location Time Lapse Photogrammetric Rock Slope Monitoring System. Remote Sens-Basel11, 1890.. https://doi.org/10.3390/rs11161890

Lazar, A., Beguž, T., Vulič, M., 2018. Monitoring of the Belca rockfall. Acta Geotechnica Slovenica 15, 2-15.. https://doi.org/10.18690/actageotechslov.15.2.2-15.2018

Li, A., Xu, N., Dai, F., Gu, G., Hu, Z., Liu, Y., 2018. Stability analysis and failure mechanism of the steeply inclined bedded rock masses surrounding a large underground opening. Tunn Undergr Sp Tech 77, 45-58.. https://doi.org/10.1016/j.tust.2018.03.023

Loew, S., GISCHIG, V., WILLENBERG, H., ALPIGER, A., MOORE, J.R., 2012. 24 Randa: Kinematics and driving mechanisms of a large complex rockslide. Landslides: Types, Mechanisms and Modeling 297-309.

Loew, S., Gschwind, S., Gischig, V., Keller-Signer, A., Valent, G., 2017. Monitoring and early warning of the 2012 Preonzo catastrophic rockslope failure. Landslides 14, 141-154.. https://doi.org/10.1007/s10346-016-0701-y

Magnin, F., Deline, P., Ravanel, L., Noetzli, J., Pogliotti, P., 2015. Thermal characteristics of permafrost in the steep alpine rock walls of the Aiguille du Midi (Mont Blanc Massif, 3842 m a.s.l). The Cryosphere 9, 109-121.. https://doi.org/10.5194/tc-9-109-2015

Magnin, F., Krautblatter, M., Deline, P., Ravanel, L., Malet, E., Bevington, A., 2015. Determination of warm, sensitive permafrost areas in near-vertical rockwalls and evaluation of distributed models by electrical resistivity tomography. J Geophys Res-Earth 120, 745-762.. https://doi.org/10.1002/2014JF003351

Ma, C., Li, T., Zhang, H., 2020. Microseismic and precursor analysis of high-stress hazards in tunnels: A case comparison of rockburst and fall of ground. Eng Geol 265, 105435.. https://doi.org/10.1016/j.enggeo.2019.105435

Marmoni, G.M., Fiorucci, M., Grechi, G., Martino, S., 2020. Modelling of thermo-mechanical effects in a rock quarry wall induced by near-surface temperature fluctuations. Int J Rock Mech Min 134.. https://doi.org/https://doi.org/10.1016/j.ijrmms.2020.104440

Matano, F., Pignalosa, A., Marino, E., Esposito, G., Caccavale, M., Caputo, T.), Sacchi, M., Somma, R., Troise, C., De Natale, G., 2015. Laser Scanning Application for Geostructural analysis of Tuffaceous Coastal Cliffs: the case of Punta Epitaffio, Pozzuoli Bay, Italy. Eur J Remote Sens48, 615-637.. https://doi.org/10.5721/EuJRS20154834

Matsuoka, N., 2008. Frost weathering and rockwall erosion in the southeastern Swiss Alps: Long-term (1994–2006) observations. Geomorphology (Amsterdam) 99, 353-368.. https://doi.org/10.1016/j.geomorph.2007.11.013

Matsuoka, N., 2019. A multi-method monitoring of timing, magnitude and origin of rockfall activity in the Japanese Alps. Geomorphology (Amsterdam) 336, 65-76.. https://doi.org/10.1016/j.geomorph.2019.03.023

Pappalardo, G., Mineo, S., Zampelli, S.P., Cubito, A., Calcaterra, D., 2016. InfraRed Thermography proposed for the estimation of the Cooling Rate Index in the remote survey of rock masses. Int J Rock Mech Min (1997) 83, 182-196.. https://doi.org/10.1016/j.ijrmms.2016.01.010

Nishii, R., Matsuoka, N., 2010. Monitoring rapid head scarp movement in an alpine rockslide. Eng Geol 115, 49-57.. https://doi.org/10.1016/j.enggeo.2010.06.014

Pappalardo, M., D'Olivo, M., 2019. Testing A Methodology to Assess Fluctuations of Coastal Rocks Surface Temperature. J Mar Sci Eng 7, 315.. https://doi.org/10.3390/jmse7090315

Pasten, C., M. García, M., Cortes, D.D., 2015. Physical and numerical modelling of the thermally induced wedging mechanism. Geotech Lett 5, 186-190.

Pratt, C., Macciotta, R., Hendry, M., 2019. Quantitative relationship between weather seasonality and rock fall occurrences north of Hope, BC, Canada. Bulletin of Eng Geol and the Environment 78, 3239-3251.. https://doi.org/10.1007/s10064-018-1358-7

Racek, O., Blahůt, J., Hartvich, F., 2021. Monitoring of thermoelastic wave within a rock mass coupling information from IR camera and crack meters: a 24-hour experiment on “Branická skála” Rock in Prague, Czechia, in: Understanding And Reducing Landslide Disaster Risk: Volume 3 Monitoring And Early Warning. Springer International Publishing, Cham.

Racek, J., 2020. Use of rock mass classifications for rock fall susceptibility analysis in the conditions of the Bohemian Massif (Bachelor thesis). Praha.

Ravanel, L., Magnin, F., Deline, P., 2017. Impacts of the 2003 and 2015 summer heatwaves on permafrost-affected rock-walls in the Mont Blanc massif. Sci total environ 609, 132-143.. https://doi.org/10.1016/j.scitotenv.2017.07.055

Reiterer, A., Huber, N.B., Bauer, A., 2010. Image-based point detec-tion and matching in a geo-monitoring system.. Allg. Verm.-Nachr. 117, 129–139.

Riquelme, A., Abelian, A., Tomas, R., Jaboyedoff, M., 2014. A new approach for semi-automatic rock mass joints recognition from 3D point clouds. Comput geos 68, 38-52.. https://doi.org/10.1016/j.cageo.2014.03.014

Sarro, R., Riquelme, A., Carlos Garcia-Davalillo, J., Maria Mateos, R., Tomas, R., Luis Pastor, J., Cano, M., Herrera, G., 2018. Rockfall Simulation Based on UAV Photogrammetry Data Obtained during an Emergency Declaration: Application at a Cultural Heritage Site. Remote Sens-Basel10, 1923.. https://doi.org/10.3390/rs10121923

Sass, O., Oberlechner, M., 2012. Is climate change causing increased rockfall frequency in Austria? Nat Hazard Earth Sys 12, 3209-3216.. https://doi.org/10.5194/nhess-12-3209-2012

Scaioni, M., Marsella, M., Crosetto, M., Tornatore, V., Wang, J., 2018. Geodetic and Remote-Sensing Sensors for Dam Deformation Monitoring. Sensors 18, 3682.. https://doi.org/10.3390/s18113682

Selby, M.J., 1980. A rock mass strength classification for geomorphic purposes: with tests from Antarctica and New Zealand. Z Geomorphol 24, 31-51.

Tertium technology, 2019. Gego Crack meter. Pisa Italy.

Thiele, S. Grose, L., Micklethwaite, S., 2018. Compass: A CloudCompare workflow for digital mapping and structural analysis, in: Eguga. p. 5548.

Tripolitsiotis, A., Daskalakis, A., Mertikas, S., Hristopulos, D., Agioutantis, Z.,, Partsinevelos, P., 2015. Detection of small-scale rockfall incidents using their seismic signature.. Third International Conference on Remote Sens-Baseland Geoinformation of the Environment 9535, 1-9.

Vasile, M., Vespremeanu-Stroe, A., 2017. Thermal weathering of granite spheroidal boulders in a dry-temperate climate, Northern Dobrogea, Romania. Earth Surf Proc Land 42, 259-271.. https://doi.org/10.1002/esp.3984

Vaziri, A., Moore, L., Ali, H., 2010. Monitoring systems for warning impending failures in slopes and open pit mines. Nat Hazards 55, 501-512.. https://doi.org/10.1007/s11069-010-9542-5

Vespremeanu-Stroe, A., Vasile, M., 2010. Rock Surface Freeze-Thaw and Thermal Stress Assessment in two Extreme Mountain Massifs: Bucegi and Măcin Mts. Revista de Geomorfologie 12.

Warren, K., Eppes, M.-C., Swami, S., Garbini, J., Putkonen, J., 2013. Automated field detection of rock fracturing, microclimate, and diurnal rock temperature and strain fields. Geosci Instrum Meth 2, 275-288.. https://doi.org/10.5194/gi-2-275-2013

Weber, S., Beutel, J., Faillettaz, J., Hasler, A., Krautblatter, M., Vieli, A., 2017. Quantifying irreversible movement in steep, fractured bedrock permafrost on Matterhorn (CH). Cryosphere 11, 567-583.. https://doi.org/10.5194/tc-11-567-2017

Weber, S., Beutel, J., Faillettaz, J., Meyer, M., Vieli, A., 2018. Acoustic and micro-seismic signal of rockfall on Matterhorn., in: 5Th European Conference On Permafrost, Book Of Abstracts. Laboratoire EDYTEM, Université de Savoie Mont-Blanc, pp. 944-945.

Weigand, M., Wagner, F.M., Limbrock, J.K., Hilbich, C., Hauck, C., Kemna, A., 2020. A monitoring system for spatiotemporal electrical self-potential measurements in cryospheric environments. Geosci Instrum Meth9, 317-336.. https://doi.org/10.5194/gi-9-317-2020

Westoby, M.J., Brasington, J., Glasser, N.F., Hambrey, M.J., Reynolds, J.M., 2012. 'Structure-from-Motion' photogrammetry: A low-cost, effective tool for geoscience applications. Geomorphology (Amsterdam) 179, 300-314.. https://doi.org/10.1016/j.geomorph.2012.08.021

Yan, Y., Li, T., Liu, J., Wang, W., Su, Q., 2019. Monitoring and early warning method for a rockfall along railways based on vibration signal characteristics. Sci Rep-UK9, 6606-6606.. https://doi.org/10.1038/s41598-019-43146-1

Yavasoglu, H., Alkan, M.N., Bilgi, S., Alkan, O., 2020. Monitoring aseismic creep trends in the İsmetpaşa and Destek segments throughout the North Anatolian Fault (NAF) with a large-scale GPS network. Geosci Instrum Meth 9, 25-40.. https://doi.org/10.5194/gi-9-25-2020

Zangerl, C., Eberhardt, E., Perzlmaier, S., 2010. Kinematic behaviour and velocity characteristics of a complex deep-seated crystalline rockslide system in relation to its interaction with a dam reservoir. Eng Geol 112, 53-67.. https://doi.org/10.1016/j.enggeo.2010.01.001

FIEDLER: Elektronika pro ekologii [WWW Document], 2020.. URL https://www.fiedler.company/ (accessed 09.21.2020).